Inefficacy of n-acetylcysteine in mitigating cue-induced relapse to amphetamine

by

Troy D. Fort

B.A., Southwestern College, 2018

A THESIS

submitted in partial fulfillment of the requirements for the degree

MASTER OF SCIENCE

Department of Psychological Sciences
College of Arts and Sciences

KANSAS STATE UNIVERSITY
Manhattan, Kansas

2022

Approved by:

Major Professor
Mary E. Cain

Copyright

Abstract

Glutamatergic imbalances are characteristic of SUDs. Glutamate is maintained by a combination of astrocytic and neuronal transporters within the nucleus accumbens (ACb) and medial prefrontal cortex (mPFC) and disruptions in this homeostasis engender SUD. One transporter, the cysteine-glutamate exchanger (xCT), is primarily localized on astrocytes and helps maintain glutamate concentrations. This process is disrupted by cocaine use, and the therapeutic *N*-acetylcysteine (NAC) lowers cue-induced relapse to cocaine by restoring xCT function. However, little research has shown how these effects extend to other psychostimulants, such as amphetamine (AMP). In the present study, we assessed disruption of astrocytic xCT expression following AMP-induced cue seeking, and the degree to which NAC can attenuate relapse via changes to astrocyte and xCT expression. To test this question, we administered NAC (100 mg/kg ip) daily during a 14-day abstinence period following completeion of amphetamine self-administration. Cue-induced relapse was tested following one (WD1) and 14 days (WD14) of withdrawal in separate subsets of animals. We then assessed expression of xCT and astrocyte densities in the mPFC and ACb.

During the relapse test, cue-induced responding was higher in AMP-treated rats compared to saline-treated rats. NAC failed to attenuate relapse at either WD 1 or WD 14. Histology indicated that rats exposed to AMP had increased astrocyte expression in the mPFC and ACb when compared AMP-naïve rats. Repeated injection with NAC decreased xCT expression within regions of the mPFC and ACb only in animals with AMP exposure. Overall, these results suggest that NAC may be an ineffective treatment option for lowering cue-induced relapse to AMP. Further, the results suggest that stimulating xCT via NAC may not be an effective therapeutic approach for decreasing cue-seeking for AMP.

Table of Contents

List of Figures

List of Tables

Acknowledgements

Quite simply, this project would not have been possible if not for the help of so many wonderful people. Though my words fall miserably short, I shall do my best to outline them here. First and foremost, I am thankful for my wife, Quinlan. Your love, support, and effort has allowed me the freedom to pursue this career path. You have been there every step of this journey, to celebrate, to listen, you've done it all and I am certainly one lucky man to have you during this process. Second, thank you to my advisor Dr. Mary Cain for her guidance, patience, and effort in helping me to complete this project during a couple of the most unprecedented years in my life. Thirdly, to the undergraduate researchers of the Cain Lab. Particularly, Taylor Stephens for her assistance in histology and sectioning. Fourthly, to my fellow graduate student peers, specifically Dylan Laux for his assistance in surgeries, and consistent support. It is a joy and a privilege to get to work with such diligent and determined students and peers. Importantly, thank you to my parents, Doug and Deanne, who have engrained in me so many qualities: diligence, integrity, and thoughtfulness come to mind. These qualities are fundamental to who I am both as an individual and as a scientist. Finally, my sisters, Chelsea and Hayley, who have always been there to inspire, to laugh, and to celebrate with me.

Chapter 1 - Introduction

Background and Significance

Psychostimulant overdoses, such as amphetamine and dextroamphetamine (Adderal) have increased by 22.3% annually from 2008 to 2017 (Kariisa, Scholl, Wilson, Seth, & Hoots, 2019). This surge in amphetamine abuse is especially prevalent in college-aged individuals (Brandt, Taverna, & Hallock, 2014). Importantly, this population is of significant concern due to the ongoing and dynamic changes in synaptic pruning and neuroplasticity that occur during late adolescence (Brown, Tapert, Grandholm, & Delis, 2000). Recent data have shown that amongst college students, psychostimulants constitute 73% of all non-medical drug use. Of those individuals, 81.2% reported non-prescription Adderall use, thus making dextroamphetamine the most commonly abused psychostimulant in this age demographic (Brandt, Taverna, & Hallock, 2014). Therefore, it is critical for us to characterize the biological mechanisms that perpetuate amphetamine-use disorder.

Recurring Episodes of Abstinence and Relapse

Addiction is a chronic disorder characterized by repeated episodes of abstinence and relapse. The drug-craving that ultimately leads to relapse remains a key obstacle in treatments designed to attenuate relapse and SUDs. Drug craving is often induced through drug-associated cues which increase motivation to obtain drug-associated outcomes, referred to here as cue-induced craving. Even after long periods of drug abstinence, drug-associated cues are still able to induce relapse, thus perpetuating addiction. Further exacerbating this issue is the finding that cue-induced drug craving increases concurrently with drug abstinence. There is a broad wealth of literature indicating that cue-induced craving increases linearly with the duration of drug

abstinence. This relationship between the increase in the motivational impact of drug-associated cues and drug abstinence is referred to as *incubation of drug craving* (Pickens et al., 2011; Grimm, Hope, Wise & Shaham, 2001; Wolf, 2016).

Though incubation of drug craving has been noted in human clinical settings (Hunt et al., 1971; Pickens et al., 2011), rodent models of addiction are often used to assess the degree to which drug-craving incubates or intensifies across the duration of drug abstinence. In such studies, animals are trained to self-administer a drug by performing an operant response (e.g. a nose poke or lever press) and are rewarded with an infusion of the drug reinforcer. However, the relationship between the operant response and the drug infusion, often referred to as a "response-outcome" relationship, only explains a portion of this issue. Stimuli present before or during the delivery of the drug can also become associated with the drug itself through Pavlovian-instrumental transfer. As such, these cues accrue associative value through incentive salience, a value which elicits "wanting" and concomitant drug-seeking behaviors when drug-cues are present (Everitt & Robbins, 2005).

The ability of the cue to induce drug-seeking is then assessed via a cue-seeking test in which active-lever pressing results in the presentation of the drug-cue, but no delivery of the drug itself. In some cases, the behavior will be extinguished after acquisition. The ability of the cue to elicit drug-seeking behavior is then assessed via a cue-induced reinstatement test. In other cases, the response-outcome relationship is never extinguished. Instead, following acquisition and self-administration sessions, animals enter an abstinence period in which they are not allowed access to the drug, self-administration chambers, or drug-associated cues. The ability of the cue to elicit drug-seeking behaviors is then assessed via a cue-induced relapse test in which active lever pressing results in the presentation of drug-associated cues, but no delivery of the

drug itself (Wolf, 2016). A wealth of research has shown that the impact that these drug-associated cues have on the motivation to perform drug-seeking behaviors increases concurrently with the duration of forced abstinence using both the reinstatement and relapse models of drug craving (Pickens et al., 2011; Grimm, Hope, Wise & Shaham, 2001; Wolf, 2016).

While both the reinstatement and relapse models are valid models of addiction and cue-seeking, the relapse model, in which the operant drug-seeking response is never extinguished, has a number of advantages over the former model of drug self-administration. First, the relapse model shows greater translational validity when compared to the reinstatement model. For instance, human addicts rarely receive extinction training for specific drug-cues during in-patient, or out-patient drug rehabilitation (Monti & MacKillo, 2007; Murray, Lacoste & Belin, 2016). Rather, rehabilitating addicts are typically required to maintain drug abstinence and then return to society, often presented with a myriad of cues that were formerly associated with drug-related behaviors. Second, extinction is not well-suited to understanding the underlying mechanisms of how Pavlovian-conditioned cues elicit relapse, as extinction training itself has been shown to induce changes in plasticity of neural circuity associated with reward-based processing (Wolf, 2016). In this light, extinction can be seen as a "relearning" of new associations rather than a permanent erasure of the previous engram which would otherwise result in "unlearning" (Bouton, 1994; Berman & Dudai, 2001). Rather than forgetting that a certain response leads to a certain outcome, one can learn the new association that the relevant stimulus no longer elicits the previous outcome.

Neurobiology of Cue-Induced Relapse and Craving

A number of drugs of abuse stimulate the mesocorticolimbic pathway, a pathway intimately involved in reward processing and learning. Everitt and Robbins (2005) have suggested that the mesocorticolimbic circuit is responsible for demarcating the transition from substance use to substance abuse through the influence of intervening stimuli associated with drug-taking. Therefore, it seems that the neural properties that make this system well-suited to associative learning also contribute to deleterious drug-seeking behaviors.

The role that dopamine (DA) plays in addiction and drug-seeking has long been a topic of investigation in the field of addiction science (Berridge & Robinson, 1998; Kelley, 2004). Indeed, the rewarding effect of addictive drugs stimulate DA release, ultimately resulting in increased reward learning and deleterious drug-seeking behaviors. The pervasive nature of chronic relapse in addicts is largely a result of neuroadaptations of dopaminergic axons in the mesocorticolimbic circuit (Kalivas, 2009). However, the last decade has a seen a shift in focus towards increasing understanding of the neruocircuity governing dopaminergic signalling within the mesocorticolimbic pathway. Particulary, the study of glutamatergic neurotransmission in the mesocorticolimbic cirtcuit is a burgeoning field for understanding how disruptions or alterations in glutamate and its' associated mechanisms can lead to drug-seeking. This shift is largely due to the perspective that the pervasive changes is dopaminergic signalling and concomitant increases in drug-seeking behavior are a consequence of long-term changes in the neurocircuitry that house these dopamine axons (Kalivas, 2009). Stated differently, researchers investigating the role of glutamate within this pathway have started to view dopamine as a consequence of long-term changes in the glutamate axons which are the proximal issue governing dopamine release in this pathway.

While corticostriatal projections are implicated in generating learned behaviors (e.g. drug-taking), these same projection neurons are also responsible for helping to modulate behavior in response to changes in environment (Kelley, 2004). In the case of pathological addiction, this behavioral phenotype can be seen as an inability to control drug-seeking in response to drug-associated cues. Kalivas (2009) and other colleagues have suggested that this pathology could arise from two primary sources in the corticostriatal system. First, addiction could arise from a maladaptive strengthening of drug-seeking behaviors. Second, addiction could also arise from deficiencies in the ability to control drug-seeking behaviors in response to drug cues. While these two potential sources of addiction point to different structures in the mesocorticolimbic system, both are likely implicated in the initiation and maintenance of addiction.

Disruptions in glutamatergic signaling in the medial prefrontal cortex (mPFC), nucleus accumbens (ACb), ventral tegmental area (VTA), orbitofrontal cortex (OFC), and the amygdala have been shown to contribute to the initiation and maintenance of cue-induced craving. The ACb primarily (90-95%) consists of GABAergic medium spiny projection neurons (MSNs) (Wolf, 2016). These medium spiny neurons help to integrate corticostriatal glutamatergic inputs, which play a pivotal role in generating motivated behaviors, and relaying information to regions of the basal ganglia tasked with execution of motor movements associated with that behavior. In this light, the ACb serves as a gateway for information derived from limbic subcircuitry to elicit activation in the motor circuit (Yin and Knowlton, 2006; Groenewegen, Wright & Beijer, 1996) and is therefore critical for turning motivation into action (Wolf, 2016; Sesack & Grace, 2010; Mogenson, Jones & Yim, 1980). When novel stimuli that predict appetitive outcomes are presented, the limbic circuitry attend to information pertaining to the stimulus. Due to the

integration of the ACb, this information then elicits activation in the motor circuit, and ultimately to the execution of motor movements targeted to the attainment of the reinforcer. As stimuli continue to predict the presentation of a particular reinforcer, neuronal activity in the limbic subcircuit decreases and neuronal activity is primarily driven by the motor subcircuit (Barnes, Kubota, Hu, Jin & Graybiel, 2005; Yin & Knowlton, 2006). This motor compensation ultimately drives behaviors associated with the attainment of that reinforcer to become increasingly habitual (Yin and Knowlton, 2006; Groenewegen, Wright & Beijer, 1996). However, if stimuli or behavior no longer elicit the presentation of the reinforcer (e.g. extinction training) then the limbic subcircuit takes over control of behavior. The proper functioning of the limbic subcircuitry should make behavioral changes more amenable to changes in the environmental contingencies associated with that reinforcer (Barnes, Kubota, Hu, Jin & Graybiel, 2005; Doya, 2008). In this light, addiction can occur from an inability to adopt new behaviors in response to changes in environmental contingencies. Compulsive drug relapse occurs from the inability of the limbic subcircuitry to inhibit behavior in the presence of negative environmental contingencies (Kalivas, 2009). Instead, the maladaptive cycle of behavior in addiction suffers from overactivity of the motor subcircuit, ultimately driving habitual and compulsive drug-seeking.

Collectively, the prefrontal cortex (PFC) is crucially linked to cognitive, emotional, and motivational processes that can help guide behavior such as: attention, inhibition, and decision-making. However, while much of the work in addiction has tended to focus on the motivational aspects, addiction is undoubtedly a disorder that involves a disruption of the balance between motivation and self-regulation (Moorman, James, McGlinchey & Aston-Jones, 2015). As I have previously indicated, inhibiting drug-seeking in response to the presentation of drug-associated

cues is one of the primary hurdles in treating addiction. Activity of the PFC has been found to be positively correlated with individuals' self-reported craving of cocaine, nicotine, and alcohol (Bonson et al., 2002; Heniz et al., 2004; Yalachkov et al., 2009). Importantly, Volkow et al. (2010) has shown that the PFC is critically involved in modifying behavior in response to drug-cues. Control participants were not instructed to inhibit their craving and showed PFC activity that positively correlated with their self-reported craving levels. Conversely, instructing addicts to suppress their craving in response to cocaine-related images resulted in a significant reduction in the activation of the right OFC as structure critical in processing visual cues, and significant activation of the right inferior frontal gyrus, a structure linked to inhibitory control (Goldstein & Volkow, 2011). However, the PFC contributes to numerous different aspects of addiction, from motivation and craving, to behavioral restraint in response to drug-craving. This diversity is due, in large part, to the heterogeneous organization the PFC, with different subregions contributing to separate aspects of addiction (e.g. motivation, attention, restraint, etc.).

The rodent medial prefrontal cortex (mPFC) receives dopaminergic input from the VTA and other limbic structures such as the amygdala and hippocampus. These inputs help the mPFC to monitor the motivational significance and salience of drug-related stimuli, thus making it a crucial component of the mesocorticolimbic pathway (Kalivas, 2009; Lasseter et al., 2010). The mPFC then uses this information to control and direct cue-induced drug-seeking via the ACb and motor structures of the basal ganglia, particularly the caudate and putamen of the dorsal striatum (Kalivas, 2009; Lasseter et al., 2010; Vertes, 2004). Recent evidence has shown that cocaine infusions to mPFC increases cocaine-seeking behaviors while inactivating the mPFC can attenuate cocaine-seeking in both cocaine reinstatement and conditioned place-preference paradigms (MaFarland & Kalivas, 2001; Capriles et al., 2003; Fuchs, et al., 2005). However,

inactivation of the mPFC has also been shown to hasten the acquisition of cocaine-taking during operant self-administration, further demonstrating the complex nature of the mPFC circuitry (Weissenborn et al, 1997).

The ventral subregion of the mPFC can be divided into the prelimbic (PL) and infralimbic (IL) cortices. These two regions are highly dissociable due to differences in their afferent projections to other brain areas associated with reward-based processing, particularly the ACb (Vertes, 2006). The majority of PL afferents project to the ACb core while IL afferents project to the ACb shell. Both PL and IL regions also show dissociable behavioral roles with the PL being pivotal for the execution of behavior, while the IL is vital for response inhibition (Gass & Chandler, 2013; Van den Oever et al., 2010). The role of PL in addiction was elucidated by the finding that pharmacological activations (i.e. muscimol, baclofen) of PL generally decrease cocaine-seeking, thus demonstrating that PL plays a pivotal role in drug-seeking (Di Pietro et al., 2006). Additionally, lesioning PL has shown to decrease reinstatement of drug-seeking following drug abstinence (Pelloux et al., 2013). The control that PL exerts over reinstatement is due to glutamatergic projection neurons to the ACb core. Indeed, cocaine-primed reinstatement has shown to increase glutamate concentrations within the ACb core, an effect which is inhibited by inactivation of PL (Baker et al., 2003; McFarland et al., 2003). This evidence further corroborates the link between PL- ACb core projections and the reinstatement of drug seeking. However, unlike PL, inactivation of IL does not affect cue-induced reinstatement to methamphetamine (Hiranita et al., 2006). While many could take this as evidence that IL is not involved in drug-seeking, IL has shown to be an integral component in suppressing drug-seeking. Inactivation of IL increases lever pressing and spontaneous recovery of extinguished cocaine self-administration following 28 days of forced abstinence while activation of IL

engendered significant reductions in cocaine-induced reinstatement (Peters et al., 2008). These behavioral effects are corroborated by changes in the cellular physiology of IL-ACb shell projections. Formation of silent synapses in IL-ACb shell projections occurs following withdrawal of cocaine self-administration (Ma et al., 2014).

Glutamate Homeostasis as a Molecular Basis for Incubation of Drug Craving

The incubation of drug-craving in response to drug-associated cues that occurs concurrenly with drug abstinence is largely a consequence of maladaptive neuroplasticity in the ACb (Wolf, 2016). The behavioral increase in the motivational impact of drug-associated cues is corroborated by an increase in the number of ACb neurons that respond to drug-associated cues. Indeed, drug-associated cues have been shown to elicit higher activation of neurons in the ACb core on Withdrawal Day 30 than on Withdrawal Day 1 (Hollander & Carelli, 2007), further corroborating a behavioral and neuronal link to the incubation of drug craving that occurs during drug abstinence. The ACb core has been found to contribute to incubation of drug-seeking, while the ACb shell has generally been found to contribute to escalation of drug intake (Wolf, 2016).

As discussed in the previous section, the last ten to fifteen years have seen a shift toward understanding the effects of glutamatergic signaling in the mesocorticolimbic pathway. However, this view has since expanded further still by implicating the action of glial cells in the release and eliminiation of glutamate from the synaptic and extrasynaptic space. This shift largely resulted from the finding that in *in vivo* microdialysates, extracellular glutamate levels were unaffected by pharmacological blockade of Na^+ and Ca^{2+} voltage-gated channels at the synapse (Timmerman & Westerink, 1997). This seminal finding changed a number of ways that researchers would begin to see glutamate in the mesocortioclimbic pathway. First, the fact that

extracellular glutamate remained homeostatic, despite antagonism of synaptic iGluRs, indicated that extracellular glutamate arises and is eliminated primarily through glial sources. Second, glial-derived reuptake mechanisms protect iGluRs at the synapse from exposure to extrasynaptic glutamate spillover. Third, perisynaptic metabotropic glutamate autoreceptors (mGluRs) are predominately stimulated by glial-derived extrasynaptic glutamate (Kalivas, 2009). As such, this finding reframed the traditional view of glutamatergic neurotransmission, which had seen this neurotransmission occurring via a systemic cycle of pre-synaptic glutamate release, binding of the ligand to iGluRs located on the post-synaptic cell, and elimination of residual glutamate via Na^+-dependent glutamate transporters (Herman & Jahr, 2007; Diamond & Jahr, 1997). Glutamatergic transmission and neuroplasticity are now seen as a vastly more complex system in which synaptic transmission is heavily modulated by a network of interactions with a host of extrasynaptic mechanisms. This shift ultimately led to what is now known as the, "Glutamate Homeostasis Hypothesis of Addiction" (Kalivas, 2009).

This theory implicates a number of astrocytic and synaptic glutamate transporters in the maintenance of glutamate homeostasis. See Figure 1 for a diagram of these mechanisms. These astroglial glutamate transporters and receptors work in concert to maintain the optimal level of glutamate in the synaptic and extrasynaptic spaces. One such transporter, the cysteine-glutamate exchanger (xCT), is responsible for exporting glutamate into the extrasynaptic space by exchanging one intracellular glutamate molecule for one extracellular cysteine molecule. Within the ACb, approximately 60% of all extracellular glutamate is derived from cystine-glutamate exchange (Baker, Xi, Shen, Swanson & Kalivas, 2002). Another transporter pivotal for maintaining glutamate homeostasis, the excitatory amino acid transporter, GLT1, is responsible for preventing ~90% of glutamate spillover from the synaptic to the extrasynaptic space

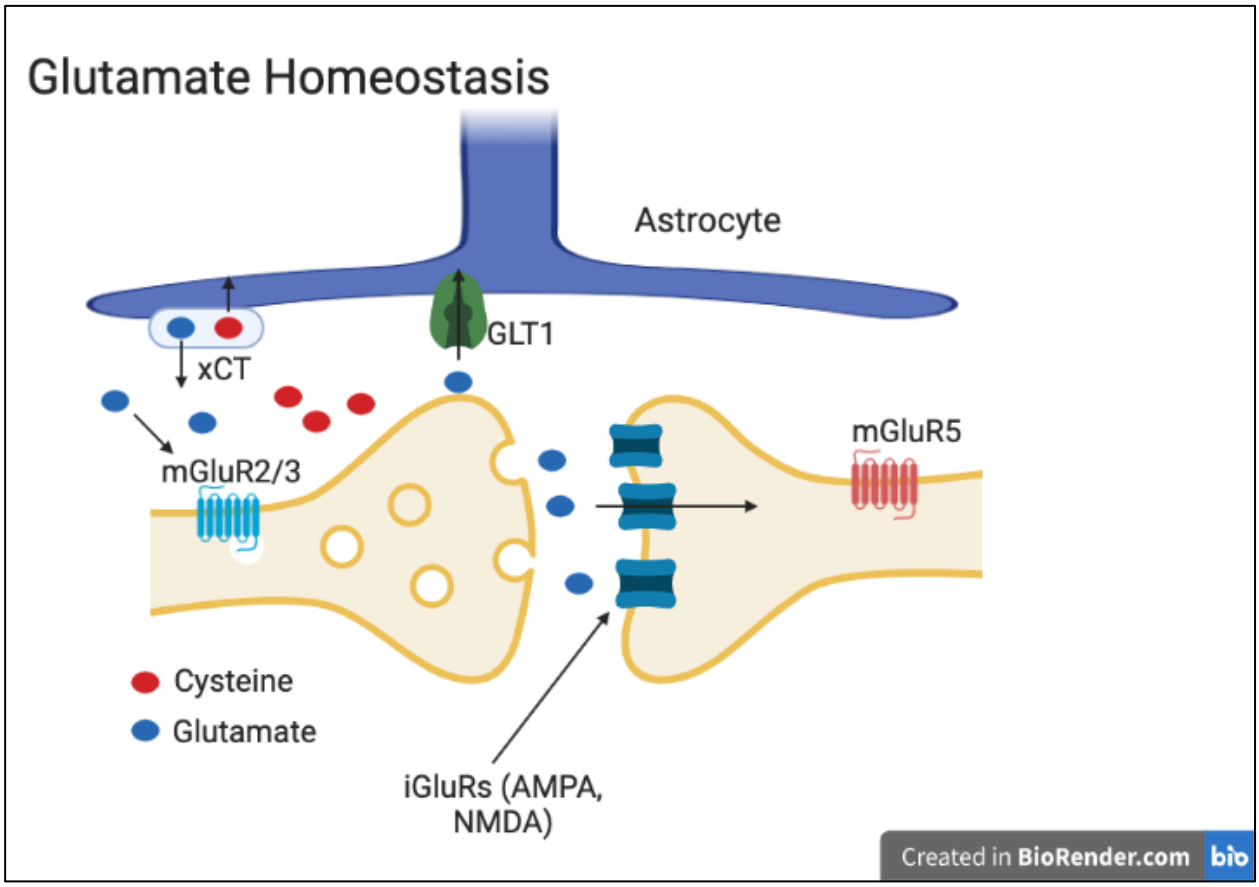

Figure 1. Simplified diagram showing optimal glutamate homeostatic conditions and mechanisms. Under optimal conditions, there is a relative balance of extrasynaptic glutamate clearance via GLT1 and export via xCT. This balance permits optimal glutamatergic tone on presynaptic mGluR2/3 autoreceptors and limited release of glutamate at the synaptic cleft. As such, optimal expression of both xCT and GLT1 produce ideal homeostatic conditions that neither permit long-term potentiation nor long-term depression at glutamatergic synapses.

(Danbolt, 2001). GLT1 is primarily localized in the synaptic cleft and aids in the buffering of ionotropic-based glutamatergic transmission (Pendyam, Mohan, Kalivas & Nair, 2009). Additionally, GLT1 traffics extracellular glutamate back to the astrocyte to await export during cysteine-glutamate exchange. Both GLT1 and xCT are primarily expressed on the surface of astrocytes, making astrocytic densities a potential indicator of putative glutamate homeostatic mechanisms (Baker, Shen, Swanson & Kalivas, 2002; Rothestein et al., 1994). Astrocytic densities can be assessed via histochemical analysis of cells expressing glial fibrillary acidic protein (GFAP), a protein which is predominately expressed on the surface of astrocytes.

Both xCT and GLT1 work in tandem to maintain optimal glutamatergic tone on synaptic iGluRs and perisynaptic mGluRs, in particular the mGluR2/3 and mGluR5 receptors. The mGluR2/3 autoreceptors are primarily localized on presynaptic neurons and are responsible for regulating synaptic glutamate release from the presynaptic neuron. When glutamate is available to bind mGluR2/3, via export of xCT on the nearby astrocyte, presynaptic glutamate release is halted. Group 1 mGluRs, such as mGluR5 are primarily located on the postsynaptic neuron and also function as a negative-feedback mechanism, helping to mediate glutamatergic release at the synapse. Similar to mGluR2/3, optimal glutamatergic tone permits mGluR5 to induce long-term depression at glutamatergic synapses via a retrograde endogenous cannabinoid signaling cascade (Moussawi et al., 2009; Kalivas, 2009).

Cocaine has been shown to downregulate the expression of both xCT and GLT1 in the mPFC and ACb (Baker et al., 2003; Knackstedt, Melendez & Kalivas, 2010; Sari, Smith, Ali & Rebec, 2009; Fisher-Smith, Houston & Rebec, 2012). This downregulation leads to a decrease in glutamatergic tone on mGluR2/3 and mGluR5, ultimately leading to disruptions in glutamate homeostasis. Therefore, agonism of mGluR2/3 and mGluR5 seem highly effective mechanisms

for preventing drug-induced neuronal potentiation which would otherwise elicit enhanced cue-induced drug-craving. The disruptions to glutamate homeostasis that occur with downregulation of xCT and GLT1 are illustrated in Figure 2. While downregulations in xCT and GLT1 are reasonably well characterized in self-administration models of cocaine and alcohol (Wolf, 2016), the potential impacts that amphetamine exposure may have on xCT and GLT1 and subsequent glutamate homeostasis are significantly less characterized. The impact that methamphetamine has on xCT and GLT1 is largely dose-dependent, with neurotoxic doses showing reductions in xCT and GLT1 while subtoxic doses may not impact GLT1 expression within the ACb during abstinence from methamphetamine (Wolf, 2016). Overall, these results show a potential departure in how glutamate homeostasis may be disrupted by different psychostimulants. It is one goal of the current experiment to explore how these glial systems, particularly xCT, may be disrupted in response to amphetamine. This knowledge will help to inform the most logical and efficacious targets for therapeutic interventions to treat cue-induced relapse to amphetamine.

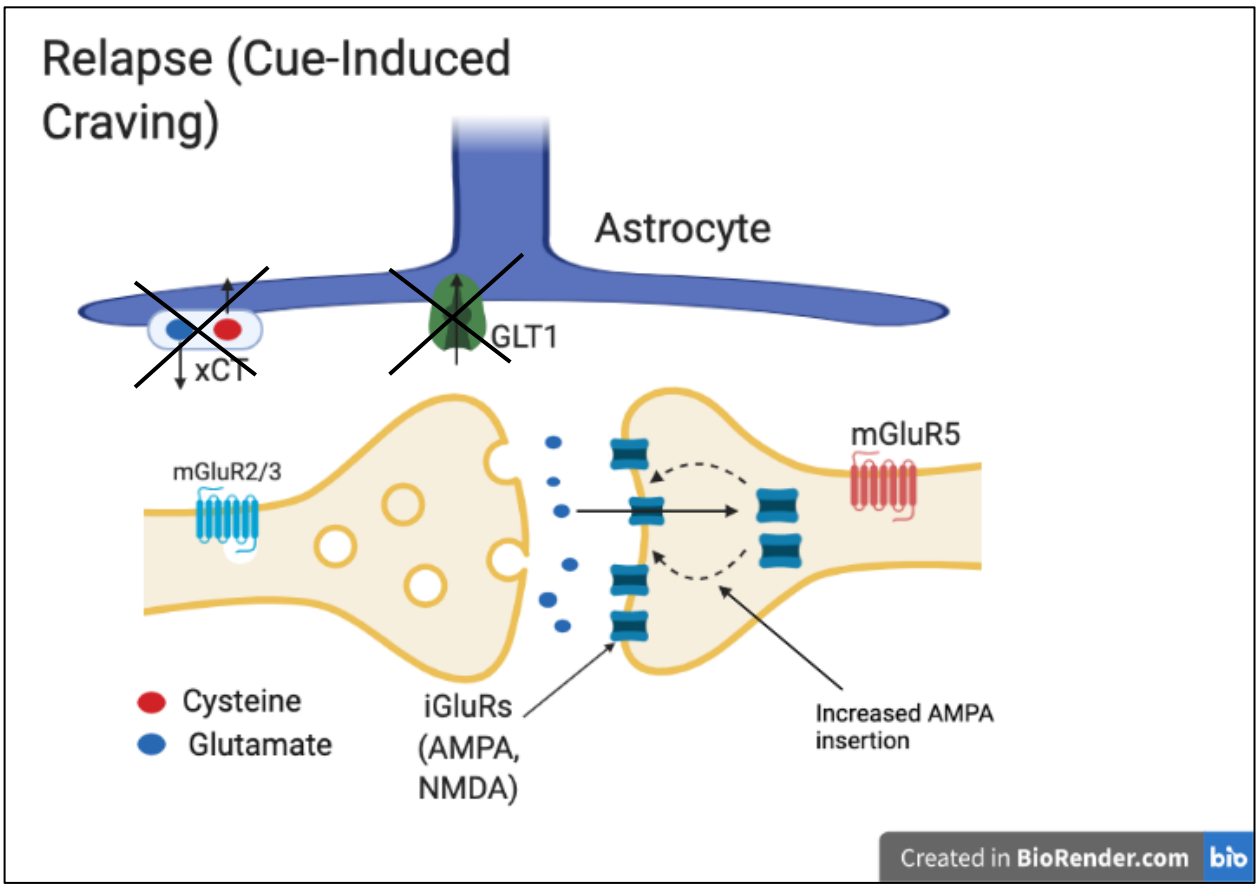

Figure 2. Simplified diagram showing disruptions in glutamate homeostasis consistent with drug abstinence and which produce increased conduced drug-craving. Under these conditions, downregulations in the surface expression of xCT and GLT1 decreases both the clearance of glutamate from the synapse by GLT1 and the export of glutamate into the extrasynaptic space by xCT. This loss in glutamate homeostasis decreases glutamatergic tone on mGluR2/3 autoreceptors. These issues have deleterious consequences and ultimately result in long-potentiation of glutamatergic synapses. Behaviorally, these maladaptive changes result in a a increase in the incentive salience of drug-related cues characteristic of cue-induced drug craving that drives relapse following protracted and acute drug abstinence.

Pharmacotherapeutic Attempts to Attenuate Cue-Induced Relapse

Therapeutics designed to restore glutamate homeostasis and attenuate associated drug-seeking have shown potential therapeutic efficacy. One such therapeutic, the β-lactam antibiotic ceftriaxone (CTX), restores the expression of GLT1 and xCT (Das et al., 2015; Knackstedt et al., 2010). Increased surface level expression of these two key glutamate transporters increases recycling of excess glutamate from the synaptic space and efflux of glial-derived glutamate via xCT into the extrasynaptic space, potentially restoring glutamate homeostasis and attenuating cue-induced craving.

Additionally, the cysteine prodrug *N*-acetylcysteine (NAC), has shown promise in mitigating cue-induced craving in both preclinical models of SUD and individuals suffering from SUD (Murray, Lacoste & Belin, 2014). While the mechanism of action underlying CTX's efficacy relies on GLT1, NAC primarily targets xCT (Knackstedt et al, 2009). NAC has been shown to attenuate decreases in extracellular glutamate that occur within the ACb core during cocaine withdrawal (Baker et al., 2003). The mechanism of action for NAC's efficacy lies in its ability to supply extracellular cysteine to stimulate xCT-mediated glutamate release. This release of extracellular cysteine via xCT is sufficient to restore glutamate homeostasis (Baker et al., 2003). This stimulation of the xCT system increases extrasynaptic glutamate levels sufficient to bind mGluR2/3, thus inhibiting presynaptic glutamate release and concomitant neuronal potentiation (Moran et al., 2005; Moussawi et al., 2009). Indeed, inhibition of xCT-mediated extracellular glutamate release precludes NAC-induced normalization of extracellular glutamate levels within the ACb core, thus suggesting that NAC-induced normalization of glutamate homeostasis is heavily reliant on xCT-mediated glutamate release (Baker et al., 2003). While the majority of research has suggested NAC's efficacy in treating cue-induced relapse to cocaine

(Reichel et al., 2011; Murray, Lacoste, & Belin, 2014), NAC has shown potential efficacy in reducing cue-induced craving for methamphetamine (Simesen et al., 2019). In summary, NAC exhibits several mechanisms of action that help demonstrate its potential utility in attenuating several aspects of glutamatergic imbalance, and most notably, in helping to mitigate cue-induced drug-seeking. However, it's efficacy in attenuating cue-induced relapse to amphetamine has not been examined.

Chapter 2 - Hypotheses

2-Hour Continuous-Access Amphetamine Self-Administration

Briefly, we predicted a robust increase in active-lever pressing for animals that self-administered amphetamine when compared to animals that self-administered the saline control.

Cue-Induce Relpase Testing

It was predicted that cue-induced active-lever responding would be increase at Withdrawal Day 14 when compared to Withdrawal Day 1 for amphetamine animals that received the saline vehicle treatment. Though incubation effects occur more consistently following extended-access self-administration (Pickens et al., 2011; Grimm, Hope, Wise & Shaham, 2001; Wolf, 2016), it was predicted that the high dose of amphetamine used here (0.1 mg/kg per infusion) would be sufficient to increase cue-induced craving at Withdrawal Day 14 compared to Withdrawal Day 1 . However, it was predicted that NAC treatment (100 mg/kg; ip) would attenuate this incubation in from Withdrawal Day 1 to Withdrawal Day 14. Additionally, we predicted that NAC would significantly lower cue-induced active-lever responding at Withdrawal Day 14, relative to the saline-vehicle treatment. Such findings would be consistent with the findings of Reichel et al. (2011) in which NAC (100 mg/kg; ip) was able to attenuate cue-induced relapse to cocaine following 14 days of forced drug abstinence.

Immunofluorescence of GFAP and xCT

I hypothesized that the mechanism of action that underscores NAC's efficacy is due to alterations in xCT expression which occur independently from astrocyte expression. I predicted that xCT expression would significantly decrease across the duration drug abstinence for

amphetamine animals treated with the saline-vehicle while xCT expression would remain unaffected in animals treated with NAC.

While I hypothesized that the efficacy of NAC will not be related to GFAP expression, I predicted that GFAP expression will be significantly altered in animals exposed to amphetamine. Specifically, I predicted that GFAP expression would significantly increase in animals previously exposed to amphetamine during self-administration compared to the animals that only self-administed saline. Such findings would be consistent with literature suggesting an increase in GFAP expression following exposure to psychostimulants (Bowers & Kalivas, 2003). Given the impact that cocaine has impairing glutamate homeostasis (Baker et al., 2003; Knackstedt, Melendez & Kalivas, 2010; Sari, Smith, Ali & Rebec, 2009; Fisher-Smith, Houston & Rebec, 2012), I predicted that previous exposure to amphetamine during self-administration would decrease xCT expression when compared to saline self-administering animals.

Chapter 3 - Methods and Materials

Animal Husbandry

Seventy-eight Male Sprague-Dawley rats were obtained from Charles River Laboratories. All rats weighed approximately 250 grams when arriving at Kansas State University. Group numbers were determined via power analysis in the statistical program G*Power. For this analysis, the alpha level was set at 0.05, the power level was set at 0.95, and the effect size was set to 0.35. The number of animals required to complete the current study exceeded what could logistically be completed in one shipment of rats. Therefore, rats from four different cohorts arrived at Kansas State University and were randomly assigned to either the amphetamine or saline self-administration conditions. All animals were pair-housed in plastic shoebox cage containing bedding and wire tops. All animals were handled weekly during scheduled cage changes. All experimental procedures were conducted in accordance with the Institutional Animal Care and Use Committee at Kansas State University and the NIH guidelines for the care and use of laboratory animals. Figure 3 shows the group sizes and assignments for all animals that met the criteria to be included in the analyses for the current study.

	NAC		VEH	
Short	**12**	**6**	**12**	**8**
Long	**12**	**8**	**12**	**8**

Figure 3. Animal numbers and group sizes for all behavioral data. These group numbers include only those rats included in the analyses because they were patent and met the response criteria. Numbers in red indicate amphetamine self-administering animal while numbers in blue indicate saline self-administering animals.

Apparatus

All training and testing was conducted in standard operant chambers (Med Associates). The standard operant chambers are enclosed within ventilated sound-attenuating chambers. Each chamber contained two levers, house light, a tone generator, a tether (to administer amphetamine; chemical-resistant tubing covered by stainless steel extension spring; the spring prevents chewing of the tubing), lights above the lever, self-administration pump, and liquid presentation magazine (dipper 0.1 ml). The opening for the magazine is 5 x 4.2 cm and this allows the rat to head poke to drink from the dipper during lever press training.

Procedures

Lever-Press Training. A figure showing a general experimental timeline can be referenced in Figure 4. After habituating to the colony for at least a week, all animals underwent several operant training sessions to facilitate the acquisition of the lever-reinforcer association. To increase motivation for water reinforcement, all animals were water-deprived for 18 hours prior to each training session. This water deprivation duration has been ubiquitously used in previous literature for lever press training (Bystrowska, Frankowska, Smaga, Pomierny-Chamiolo, & Filip, 2018; Frenk, Martin, Vitouchanskaia, Dar, & Shalev, 2017; Navarrete, Garcia-Gutierrez, & Manzanares, 2018; Sadakierska-Chudy et al., 2017; Tandon, Keefe, & Taha, 2017; Windisch & Czachowski, 2018). The reinforcer for all lever press training sessions was a presentation of 0.1 ml of water. During the first session, water access was not contingent on lever pressing. During the second training session, only one lever was presented to the animal and water reinforcement was contingent on active lever pressing. Following successfully acquisition of the lever-reinforcement contingency, all animals underwent three more fixed-ratio 1 (FR-1)

water self-administration sessions. During the three FR-1 water training sessions, all animals were presented with both the active lever, which resulted in water reinforcement, and an inactive lever which had no programmed consequence. After completion of each session, rats were returned to their home cages and were given *ad libitum* access. We did not observe weight loss or signs of dehydration in the rats during the week of water restriction and all rats readily learned to lever press.

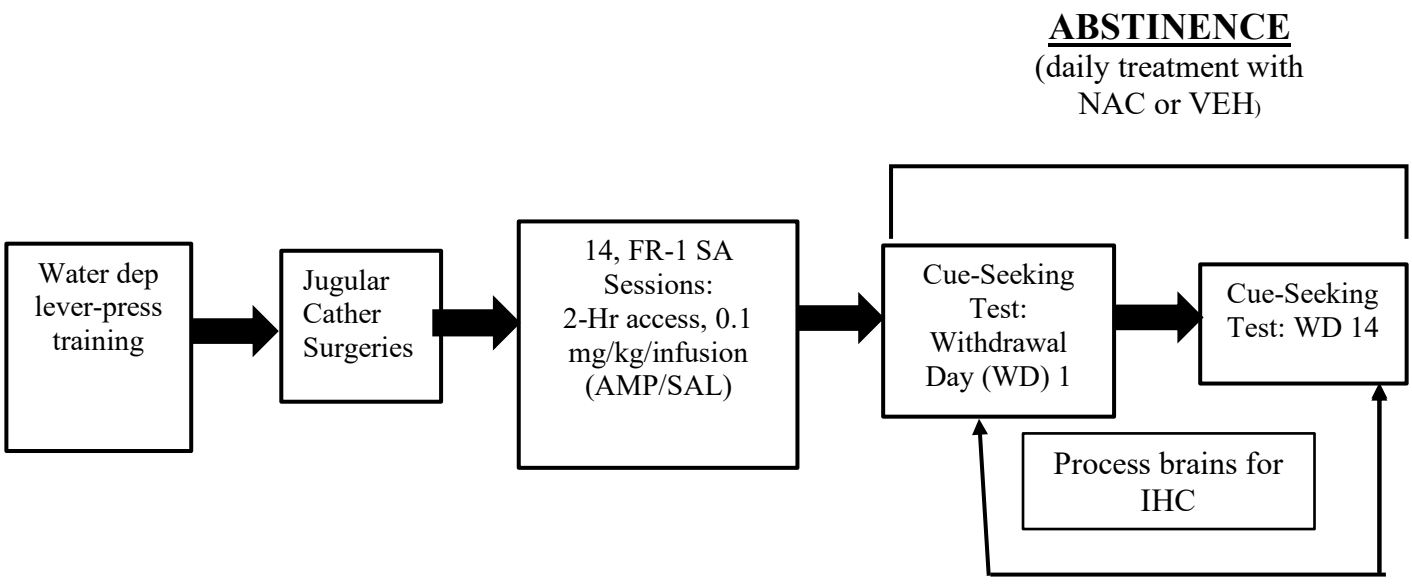

Figure 4. Experimental timeline.

Surgical Procedures. Following acquisition of lever pressing, all animals were given 3-4 days of post-training recovery. Rats were deeply anesthetized with isoflurane (~ 5%) and prepped for surgery by shaving incision sites on the animal's dorsal side and the ventral side of the neck. All incision sites were then scrubbed with chlorhexidine and isopropyl alcohol. Following preoperative care, a 3 cm horizontal incision was made approximately 6-8 cm below

the animal's scapulae. A second incision was made approximately 4 cm above the initial horizontal incision which served as a point for the catheter port to exit the animal's back. A final superficial incision was made on the ventral surface of the neck, just above and perpendicular to animal's jugular vein. Polyurethane catheters (12 cm in length, 0.2 mm internal diameter) were inserted through the dorsal incision in the animal's back, tunneled under the skin and into the animal's left jugular vein. The jugular vein was isolated inside the neck incision and a small lateral incision was made in the jugular vein using vein scissors. The catheter tubing was then inserted into the jugular vein and secured in place via suture thread. The neck incision was closed using 3M VetBond surgical glue. The horizontal incision on the back of the animal was closed via suture thread and surgical glue.

Catheter tubing was subcutaneously connected to a 22-gauge back-mounted cannula (Plastics One: Roanoke, VA) and sutured to surgical mesh (Biomedical Structures; Warwick, RI). The catheter cannula was protected by a cannula cap. To prevent animals from chewing or damaging back mounts, a stainless-steel bolt was threaded onto the end of the back mount. During the first 2 days of recovery rats were treated with Meloxicam (2.0 mg/kg after surgery;1.0 mg/kg thereafter) in order to alleviate pain. Baytril® (Enrofloxacin, 2.5% (25 mg/ml) diluted with sterile saline to a final concentration of 6-8 mg/ml administered in a 0.1 ml infusion volume) was used to prevent infection. Propofol (Methohexital 10 mg/ml @ 0.1 ml infusion) was used to check catheter patency. At this dose propofol administered intravenously causes rats to lose muscle tone and become lethargic within a few seconds of the infusion. Rats that did not display signs of a functional catheter were excluded from further analyses.

Amphetamine Self-Administration. Following 4-5 days of post-surgical recovery, all animals began 14, 2-hr fixed-ratio 1 (FR1) amphetamine self-administration sessions. During FR1 self-administration, active lever pressing resulted in a 0.1 mg/kg infusion of amphetamine administered over ~5.9 sec[1] and the concomitant illumination of the cue-light located above the active lever. Illumination of the cue-light terminated at the completion of the amphetamine infusion. Following the infusion and cue-light presentation, the houselight illuminated signaling a 20-sec timeout period during which active lever presses were recorded but were inconsequential. Similarly, inactive lever presses were recorded but had no programmed consequence. Catheter patency was re-checked before the first and following the last self-administration session via propofol infusion (10 mg/ml; 0.1-0.15 ml, i.v.). To achieve stable responding, animals were required to average 10 or more amphetamine infusions across all 14 self-administration sessions, as well as maintaining a 2:1 ratio of active to inactive-lever responses over the last 7 self-administration sessions (Arndt, Jones & Cain, 2015; Cain, Denehy & Bardo, 2008). There were no stability critera for saline self-administering animals. Data from animals in the amphetamine group with non-patent catheters or from animals that failed to meet the above stability criteria were excluded from all analyses. Five animals were excluded due to a loss of catheter patency and one animal was excluded due to failure to meet the above stability criteria.

Incubation and Cue-Induced Relapse Testing. Upon completion of 14 self-administration sessions, all animals entered a forced abstinence period. During the abstinence

[1] The infusion speed is adjusted for body weight, but the average infusion speed is approximately 5.9 seconds.

period all animals remained in their home cages and were not exposed to the drug, self-administration chamber, or drug-associated cues and received daily intraperitoneal injections of either NAC (100 mg/kg dissolved in sterile saline) or the saline vehicle. Cue-induced craving was assessed at the cessation of the abstinence period. Animals received one final injection of NAC (100 mg/kg) or the saline vehicle two hours prior to cue-induced relapse testing. During the cue-induced relapse test, the motivational impact of drug-associated cues was evaluated by reinforcing active lever presses with presentations of the previously associated drug-cue but no delivery of the drug itself. All relapse tests were 2 hours in duration and active lever presses resulted in the illumination of cue lights and houselight. Inactive lever presses were recorded but had no programmed consequence. Given that no amphetamine was available during relapse testing, no timeout period was present during the relapse test. One subset of animals underwent cue-induced relapse testing after one day of withdrawal (WD1), thus allowing us to examine the effects of drug-regulated cues following an acute abstinence period. The other subset of animals underwent cue-induced relapse testing after 14 days of withdrawal (WD14), likewise allowing us to examine the motivational impact of drug-related cues following protracted drug abstinence.

Perfusions and Immunofluorescence.

Immediately following completion of the cue-induced relapse test, all animals were humanely euthanized via sodium pentobarbitol (Sleep Away). These euthanasia procedures are consistent with the American Veterinary Medical Association (AVMA) guidelines. Following deep anesthesia, animals were transcardially perfused with 0.9% saline and 4% paraformaldehyde and brains were extracted for histochemical analysis. Following extraction, all specimens were transferred to sterilized scintillation vials containing 4% paraformaldehyde for a

4-hour post-fixation period. Following post-fixation, samples were transferred to 20% sucrose cryoprotectant. This step creates a hypertonic environment for the tissue sample to promote dehydration and preclude freezing artifacts. Following sufficient dehydration, all samples were snap-frozen on dry ice and transferred to a constant storage temperature of -80ºC until cryosectioning. Brains were sectioned at a thickness of 40 um. Sections were collected and placed serially into one of three wells (each containing cryopreservant- 20% glycerol, 2% DMSO in 1X PBS) of a 6-well plate to ensure equal distribution across the three wells. Following sectioning, all tissue was stored at -80ºC. Approximately 24 hours prior to running each immunofluorescent assay, frozen sections were placed at 4ºC to thaw gradually.

Immunoassays began by permeabilizing floating sections with 6, 5-minute rinses in PBS containing 0.2% Triton-X 100 (1X PBS-TX). Following permeabilization, free-floating sections were blocked in PBS containing 0.2% Triton-X 100 and 5% normal goat serum (Vector Laboratories: S-1000) for 30 minutes at room temperature. After blocking, sections were again subjected to 3, 5-minute rinses in PBS-TX. Free-floating sections were then simultaneously incubated in diluted unconjugated primary antibodies to assess astrocytic densities and astroglial glutamate transporter expression in the mPFC and ACb. GFAP primary antibody dilutions were prepared using a 1:2,500 dilution[2] and xCT primary antibody were prepared using a 1:200 dilution. Both primary and secondary antibodies were diluted in PBS containing 0.2% Triton-X 100. Following primary antibody incubation, sections were again subjected to 3, 5-minute rinses in PBS. Tissue was then incubated in fluorescently conjugated secondary antibodies at room temperature for 3 hours. Fluorescent-labeling of GFAP+ cells in the mPFC and ACb was

[2] This antibody dilution was informed by prior GFAP IHC-enzymatic detection (data unpublished)

assessed using Alexa Fluor 647 goat anti-chicken (1:500 dilution) fluorescent-conjugated secondary antibody. Expression and localization of xCT was assessed using Alexa Fluor 488 goat anti-rabbit fluorescent-conjugated secondary antibody (1:500 dilution). Following three hours of simultaneous incubation in both secondary antibodies, sections were again washed three times with 1X PBS. Sections were counterstained with the DAPI (dihydrochloride; Invitrogen D1306) using a 1:30,000 dilution for 10 minutes at room temperature. Following cessation of counterstaining, tissue was rinsed three final times in PBS. Free-floating sections were transferred to microscope slides and coverslipped using VectaShield coverslipping medium and coverslips were sealed using standard clear nail polish. Table 1 summarizes the dilutions and sources of each primary and secondary antibody used in this simulatenous fluorescent procedure.

Images were acquired on an Olympus BX63F fluorescence microscope located in the Behavioral Neuroscience core within the Department of Psychological Sciences at Kansas State University. Images were taken at anterior, middle, and posterior regions of each area of interest for all samples. Given that there were no significant differences in expression across the anterior-posterior axis of each region of interest, mean cell counts for each region were then derived by averaging cell counts across the three images. These aggregated cell counts were used in all immunofluorescence analyses. All image analysis was conducted in Image J. Astrocyte numbers were generated via hand counting of cells showing positive expression of both GFAP and DAPI. Expression of xCT was determined via densitometric analysis of the relative optical density after performing a background correction. This background correction allowed for us to control for any potential differences in background due to autofluorescence that can occur with GFP (wavelength of 488 nm) fluorescence channels. Given that there were no significant differences in xCT optical density across the anterior-posterior axis, the optical density values obtained from

densitometric analyses were aggregated into one value for each subject. All image quantification was conducted by individuals blind to experimental conditions.

Table 1. *Summary of reagents used in simultaneous immunofluorescence procedure.*

Antibody	Dilution (either PBS or PBS-TX as diluent)	Vendor	Identifier
Chicken anti-GFAP (polyclonal)	1:2,500	Novus Biologicals	NBP1-05198
Rabbit anti-xCT (polyclonal)	1:200	Novus Biologicals	NB300-318
Goat anti-Chicken IgY (H+L), Alexa Fluor 647	1:500	Invitrogen	A32933
Goat anti-Rabbit IgG (H+L), Alexa Fluor 488	1:500	Invitrogen	A32731

Data Analysis.

Self-administration sessions were analyzed using linear multilevel modeling. The number of active lever presses, excluding those that occurred during the 20 second timeout period, served as the primary dependent variable for all analyses. Any reference to "active-lever responding" throughout the rest of this document will mean that the measure excludes any response that occured during the timeout period. Self-administration multilevel models specified the following fixed effects: the drug that was self-administered (amphetamine or saline), session (a continuous variable consisting of 14 self-administration sessions), and a drug x session interaction, while the intercept and/or session slope of each subject was allowed to vary as random effects. Models utilizing different random effect structures (e.g. intercept or intercept and slope) were compared using Akaike's Information Criterion (AIC) to determine the optimal model. Tukey's HSD pair-

wise comparisons and simple slopes analyses were used where appropriate. Active responses that fell three standard deviations away from the grand mean were deemed outliers and were thus excluded from analysis for that session. Additional analyses comparing responding of individual cohorts were also conducted using multilevel modeling. These analyses specified the animal cohort (four level categorical variable) as a fixed effect, and specified both the intercept and session slope of each subject as random effects.

Cue-induced relapse sessions were analyzed using a three-way ANOVA. The overall number of active-lever responses served as the primary dependent variable of analysis. Cue-test ANOVAs included the main effects of drug self-administration condition (amphetamine or saline), treatment (NAC or VEH), incubation length (WD1 or WD14), and a Treatment x Incubation interaction term to assess whether the efficacy of NAC treatment is moderated by abstinence duration.

All immunofluorescent data were analyzed using three-way full factorial ANOVAs which included the main effects of Treatment (NAC, VEH), self-administration condition (amphetamine, saline), Incubation Length (Short, Long), and all possible interactions. Post-hoc power analysis indicated that statistical power was equal to 0.15 for all immunofluorescence analyses. Significance levels were set to $\alpha = .05$ for all analyses conducted.

Chapter 4 - Results

Cohort Active-Responding During 2-Hr Self-Administration

Due to the fact that the current experiment was conducted with four different cohorts of rats, cohort was included as a factor in the analyses to ensure that that there were no cohort-specific effects on amphetamine self-administration. This analysis specified both the intercept and session slope of each rat as random effects. The cohort that the rat belonged to (1-4) was specified as the lone fixed effect. This fixed effect allowed us to examine cohort-specific differences in average amphetamine self-administration occurring in the duration self-administration testing. Interestingly, the analysis revealed that there were differences in average active lever-pressing for amphetamine amongst the four self-administration cohorts, $F(3, 43) = 3.97$, $p = .01$. This effect was probed using a Tukey's HSD post-hoc test. Post-hoc examination revealed that active responding for amphetamine was significantly higher in Cohort 1 ($M = 29.12$, $SE = 1.64$, $SD = 5.19$) than in Cohort 2 ($M = 23.09$, $SE = 1.45$, $SD = 3.84$), $p = 0.04$. This cohort effect is shown graphically shown in Figure 5.

Given the cohort difference, a second analysis was conducted using only data from the second week of self-administration to confirm the cohort effect was no longer present once responding had stabilized. The intercept and session slope of each rat served as random effects while the rat's cohort (1-4) served as the lone fixed effect. This random and fixed effect structure was identical to the initial cohort analysis conducted on all active-lever pressing during self-administration sessions 1-14. The significant effect of cohort was no longer present for active-lever responding during the second week of self-administration (Sessions 8-14) , $F(3,43) = 1.53$, $p = 0.22$. Cohort active-lever responding during Sessions 8-14 are shown in Figure 6.

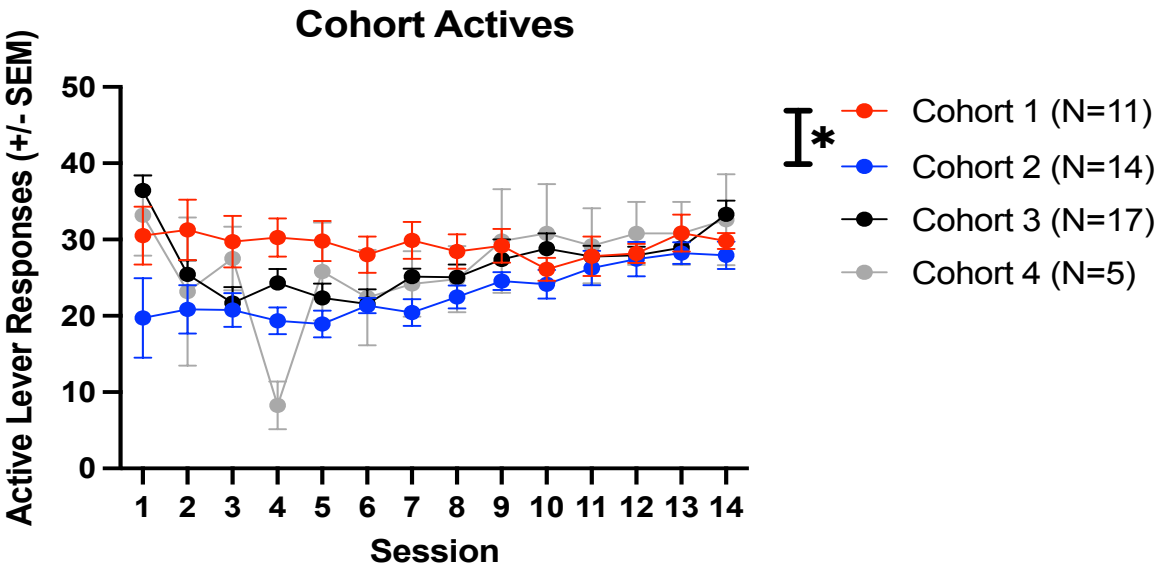

Figure 5. Mean (± SEM) active-lever responding for amphetamine (0.1 mg/kg per infusion) during 2-hr FR-1 self-administration training. The bar and asterisk indicates that mean active-lever responding was significantly higher in Cohort 1 when compared to Cohort 2, $p = .04$.

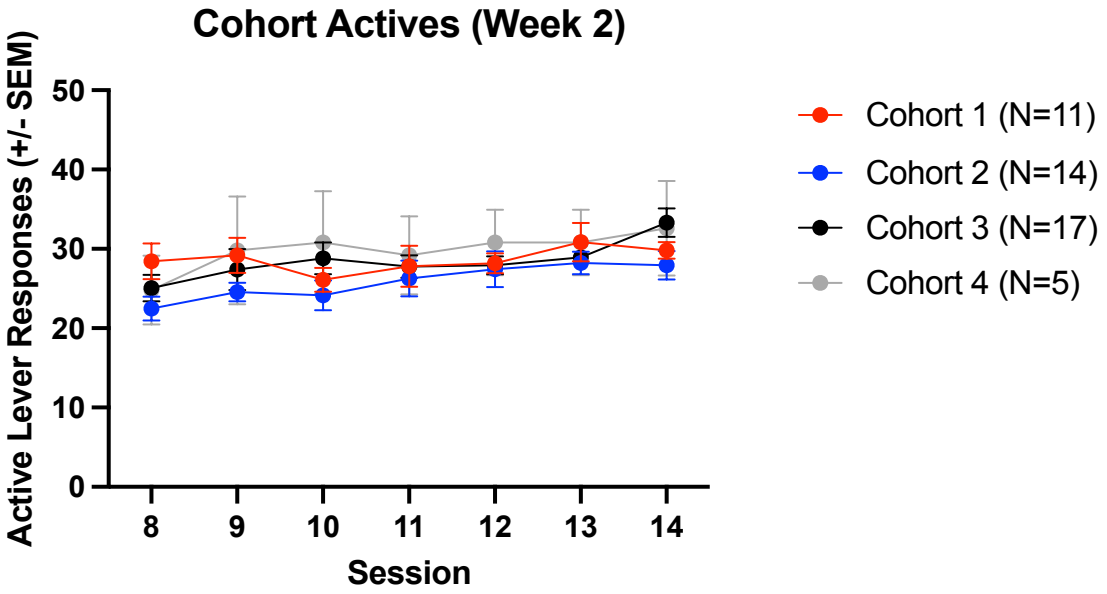

Figure 6. Mean (+/- SEM) cohort active-lever responding for amphetamine (0.1 mg/kg per infusion) when limited to the second week of amphetamine self-administration.

Active-Responding During 2-Hr Self-Administration

Linear multilevel modeling was used to examine differences in active-lever responding across the 14, 2-hr self-administration sessions. Analysis of models consisting of two different random effect structures indicated that optimal model performance occurred when both the intercept and subject slope for each session were specified as random effects. Specifying both the intercept and subject slope of each session as random effects resulted in approximately a 50-unit decrease in AIC from a model which solely specified the intercept as a random effect.

Results of the multilevel model revealed a significant fixed effect of drug self-administration condition, $F(1, 75) = 122.21$, $p < .001$, such that active-lever responding for amphetamine was significantly higher than active-lever responding for the saline vehicle (See Figure 7). Additionally, results indicate a significant fixed effect of self-administration session, $F(1, 73) = 6.24$, $p = .01$, such that active-lever responding tended to decrease over the course of the 14 self-administration sessions, when collapsed across the drug self-administration condition. More importantly, the drug (amphetamine or saline) x session interaction was a significant predictor of overall active-lever responding during self-administration training, $F(1, 73) = 21.66$, $p < .001$. Analysis of this interaction revealed that active-lever responding for amphetamine remained constant over the course of self-administration while the slope of the active-lever responding for saline decreased over the course of self-administration. As such, it seemed that the significant fixed effect of session was largely driven by decreasing self-administration in saline self-administering rats. The fixed effects of session and the drug (amphetamine or saline) x session interaction are shown in Figure 9. All model fit statistics and parameter estimates are presented in Table 2. Inactive-lever responding during 2-hr FR-1 self-administration are shown in Figure 8.

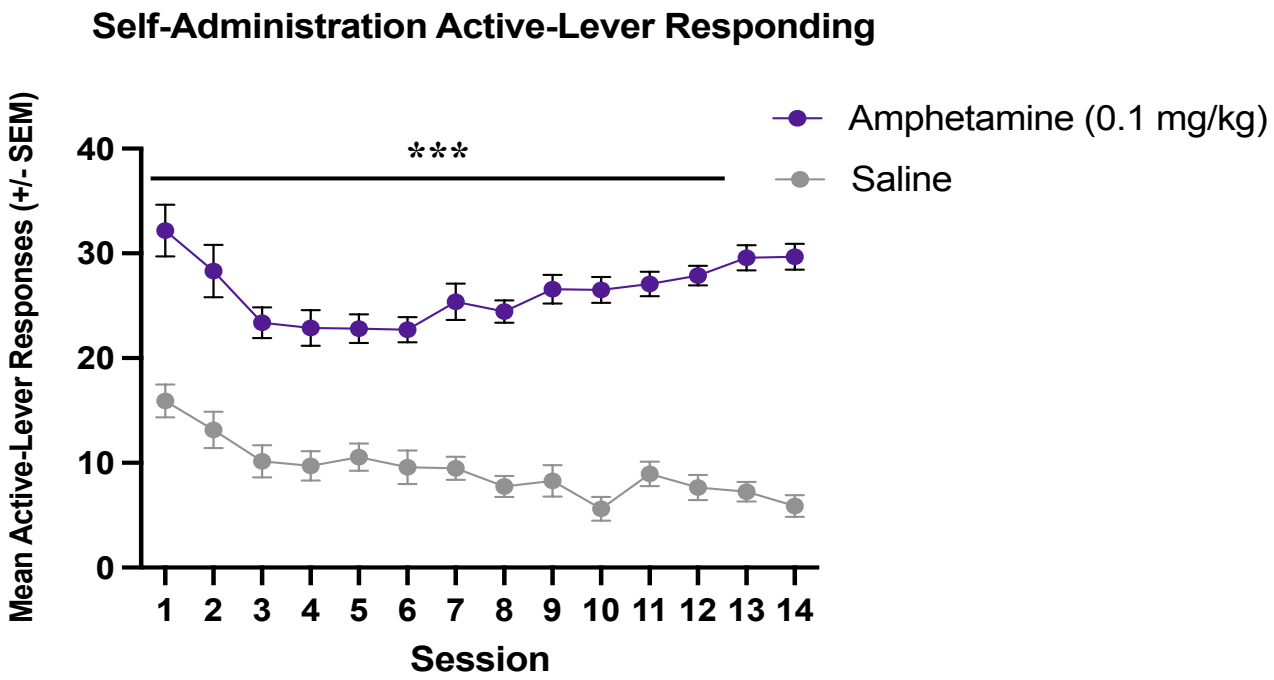

Figure 7. Mean active-lever responding (+/- SEM) for amphetamine (0.1 mg/kg per infusion) and saline during 2-hr FR-1 self-administration sessions. The bar and asterices indcate that active-lever responding was significantly higher for amphetamine when compared to saline, $p < .001$.

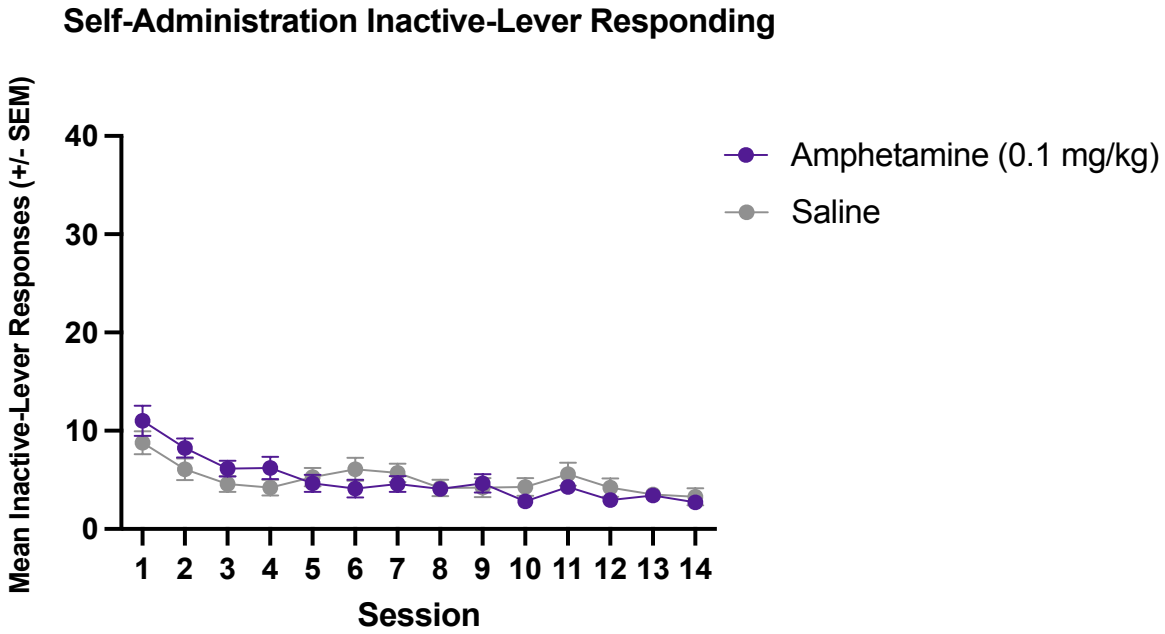

Figure 8. Mean (± SEM) inactive-lever responding during 2-hr FR-1 self-administration sessions in amphetamine and saline self-administering animals.

Table 2. *Fixed Effects and Model Fit Statistics for Self-Administration Multilevel Model Using Both Intercept and Subject Slope of Each Session as Random Effects*

					Model Statistics		
	B	*SE*	*t*	*p*	R^2	$R^2_{adjusted}$	*AIC*
Intercept	20.39	1.08	18.90	**< .001**	0.74	0.74	7324.5
Session	-0.25	0.10	-2.50	**.01**			
Drug (AMP/SAL)	8.38	0.76	11.50	**< .001**			
Drug * Session	0.47	0.10	4.65	**< .001**			

Note: Significance is indicated by boldfaced font

Active-Responding During Cue-Induced Relapse Testing

The three-way ANOVA for active-lever responding during the cue-induced relapse test indicate that there was a significant main effect of drug condition (amphetamine or saline), such that cue-induced active-lever responding was significantly greater in animals who had previously self-administered amphetamine for 14 days, $F(1, 71) = 46.31$, $p < .001$. Statistical analysis did not indicate that the Incubation Length (WD1 or WD14), Treatment (NAC or VEH), or their interaction were significant predictors of active-lever responding during cue-induced relapse testing. Average active-lever responding is shown graphically in Figure 9 . Results of the cue-induced relapse test ANOVA are summarized in Table 3.

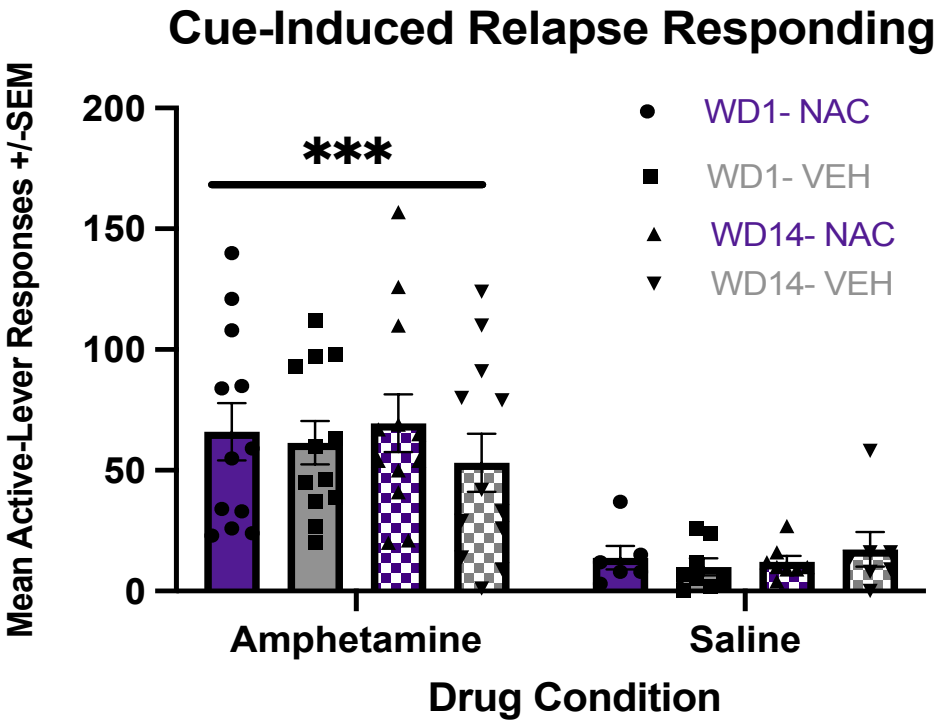

Figure 9. Mean (± SEM) cue-induced active-lever responding during the cue-induced relapse test. Bars marked in purple indicate animals that received N-acetylcysteine (NAC) during abstinence where bars marked in grey indicate animals that received injections of the saline vehicle (VEH). Solid bars indicate that animals were tested on Withdrawal Day 1 (WD1) whereas checkered bars indicate animals that were tested on Withdrawal Day 14 (WD14). The solid bar and asterices indicate that cue-induced active-lever responding was significantly higher animals that previously self-administered amphetamine when compared to those that self-administered saline. ***$p < .001$

Table 3. *Results from Three-Way Analysis of Variance of Cue-Induced Relapse Test*

	df	*SS*	*F*	*p*
Drug (AMP or SAL)	1	45462.16	46.31	**< .001**
Incubation (WD1 or WD14)	1	11.48	0.01	.91
Treatment (NAC or VEH)	1	458.54	0.47	.50
Incubation * Treatment	1	5.16	0.01	.94
Error	71	69,701.62	981.7	
Total	75	115,961.93		

Note: Significance is indicated by boldfaced font

Immunofluorescence of GFAP Within the Nucleus Accumbens

Two separate three-way ANOVAs were conducted to assess GFAP+ cell expression within the ACb core and shell. Within the ACb core, results indicated a significant main effect of drug self-administration condition (amphetamine or saline), such that higher GFAP+ cell expression were seen in animals with a history of amphetamine self-administration, $F(1, 32) = 9.47$, $p = .004$. Similarly, amphetamine self-administration was shown to increase GFAP+ cell expression in the ACb shell, $F(1, 32) = 7.32$, $p = .01$. These effects are shown graphically in Figure 10. Representative 20X images from the ACb core and shell can be seen in Figures 11 and 12, respectively. Results of both ACb ANOVAs are summarized in Tables 4 and 5.

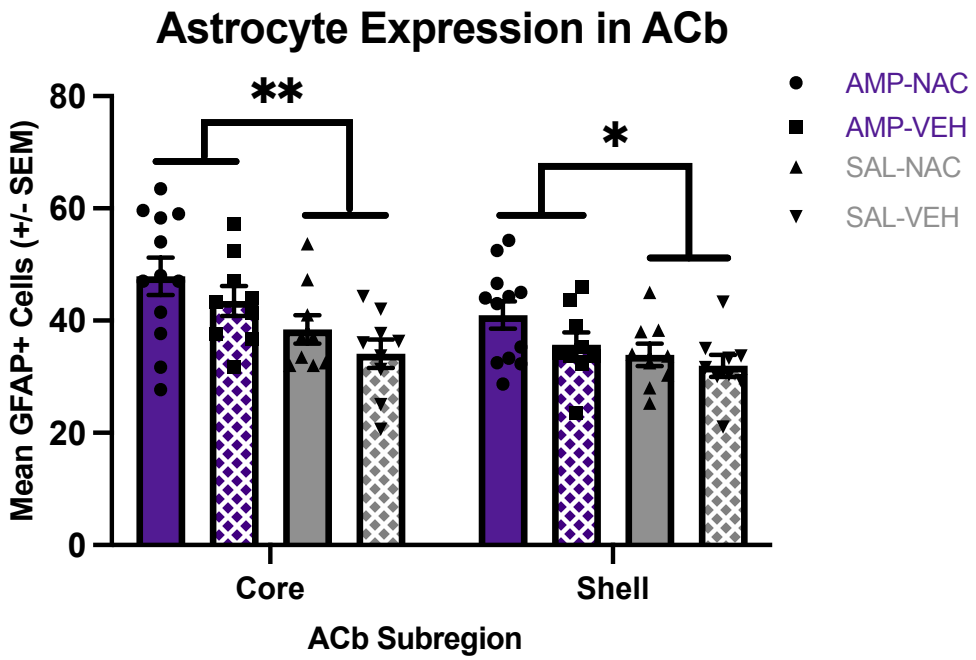

Figure 10. Mean GFAP+ cell expression (+/- SEM) within the ACb core and shell. Purple bars indicate animals that previously self-administered amphetamine (AMP) whereas grey bars indicate animals that previously self-administered saline (SAL). Solid bars indicate animals that received injections of N-acetylysteine (NAC) during abstinence and checkered bars denote animals that received injections of the saline vehicle (VEH). Bars and asterices indicate greater GFAP+ cell expression in amphetamine self-administering animals when compared to saline. ** indicates that $p < .01$, * indicates that $p < .05$

Table 4. *Results from Three-Way Analysis of Variance of Astrocyte Expression Within ACb Core*

	df	*SS*	*F*	*p*
Drug (AMP or SAL)	1	802.38	9.47	**.004**
Incubation Length (WD1 or WD14)	1	88.10	1.04	.32
Treatment (NAC or VEH)	1	292.87	3.46	.07
Incubation * Treatment	1	87.31	1.03	.32
Incubation * Drug	1	34.32	.40	.53
Treatment * Drug	1	1.15	.01	.91
Incubation * Treatment * Drug	1	5.83	.07	.79
Error	32	2712.44		
Total	39	4014.29		

Note: Significance is indicated by boldfaced font

Table 5. *Results from Three-Way Analysis of Variance of Astrocyte Expression Within ACb Shell*

	df	*SS*	*F*	*p*
Drug (AMP or SAL)	1	321.94	7.32	**.01**
Incubation Length (WD1 or WD14)	1	158..47	3.60	.07
Treatment (NAC or VEH)	1	139.01	3.16	.08
Incubation * Treatment	1	73.94	1.68	.20
Incubation * Drug	1	75.39	1.71	.20
Treatment * Drug	1	21.24	.48	.49
Incubation * Treatment * Drug	1	3.77	.09	.77
Error	32	1407.45		
Total	39	2223.72		

Note: Significance is indicated by boldfaced font

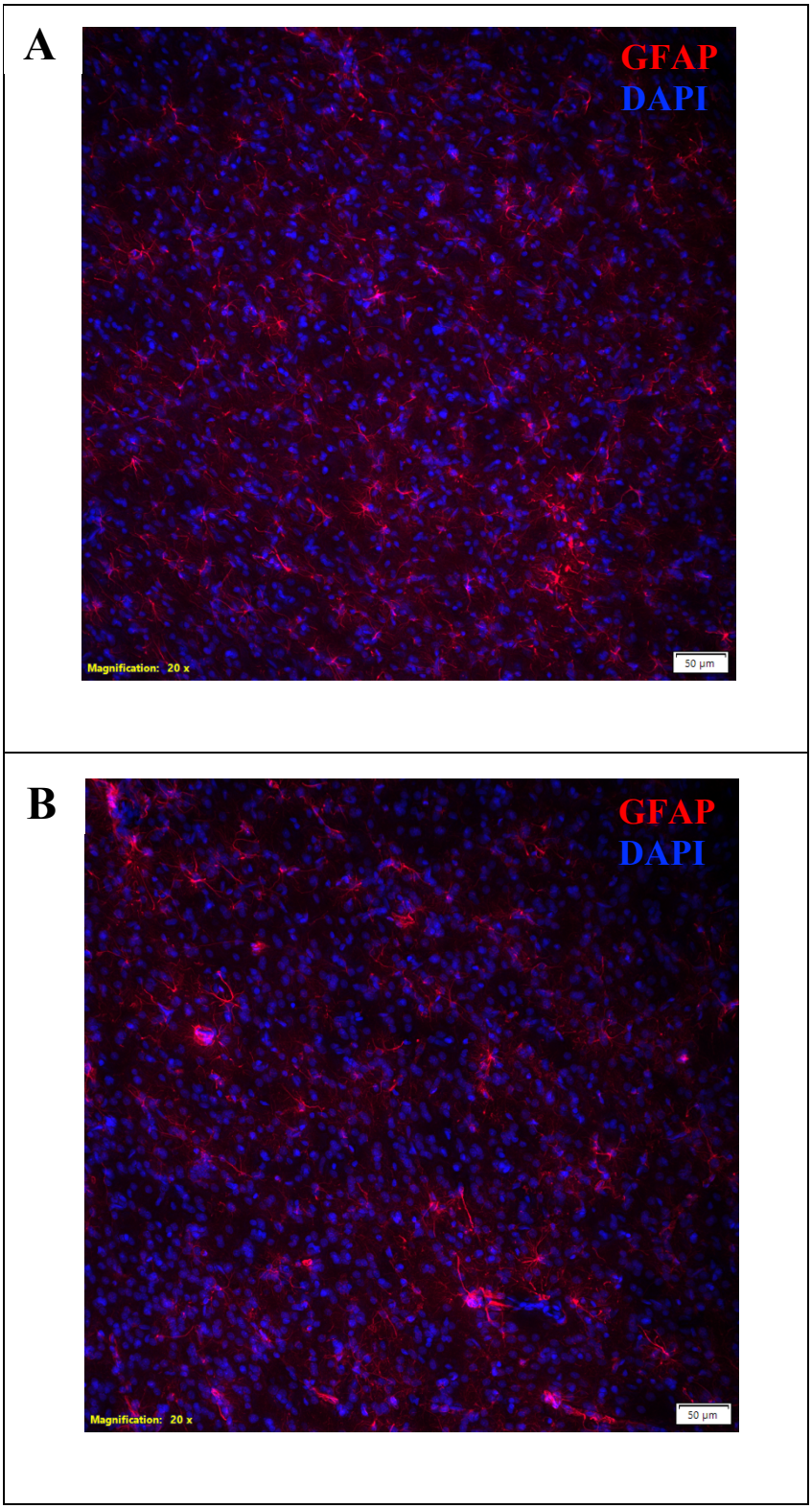

Figure 11. Representative 20X images of GFAP (astrocyte) and DAPI colocalization in the ACb core. (A) Representative image showing high GFAP expression, as quantified by cells showing both GFAP and DAPI expression. (B) Representative image showing low GFAP expression.

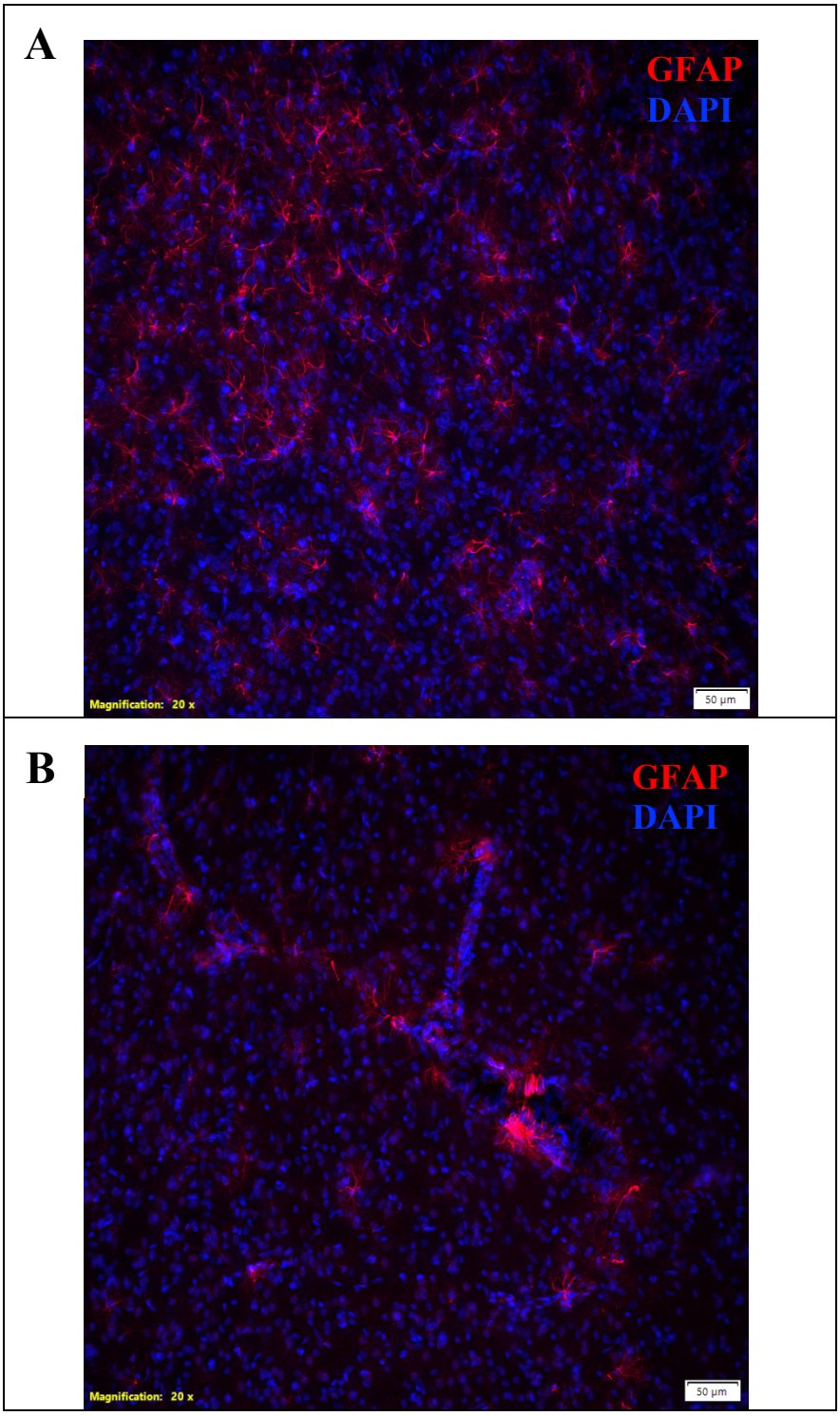

Figure 12. Representative 20X images of GFAP (astrocyte) and DAPI colocalization in the ACb shell. (A) Representative image showing high GFAP expression, as quantified by cells showing both GFAP and DAPI expression. (B) Representative image showing low GFAP expression.

Immunofluorescence of GFAP Within the Medial Prefrontal Cortex

Two separate three-way ANOVAs were conducted to determine GFAP+ cell expression within the prelimbic (PL) and infralimbic (IL) cortices of the medial prefrontal cortex (mPFC). Within the PL, results showed a significant main effect of drug self-administration condition, such that amphetamine-treated animals showed increased GFAP+ cells, $F(1, 33) = 62.06$, $p < .001$. A similar effect was shown in IL, within amphetamine increasing GFAP+ cell expression when compared to saline self-administration, $F(1, 33) = 39.09$, $p < .001$. Analysis did not indicate any other significant main effects or interactions within the PL or IL. These effects are shown graphically in Figure 13. Representative 20X images from the PL and IL cortices can be seen in Figures 14 and 15, respectively. Results from both mPFC ANOVAs are summarized in Tables 6 and 7.

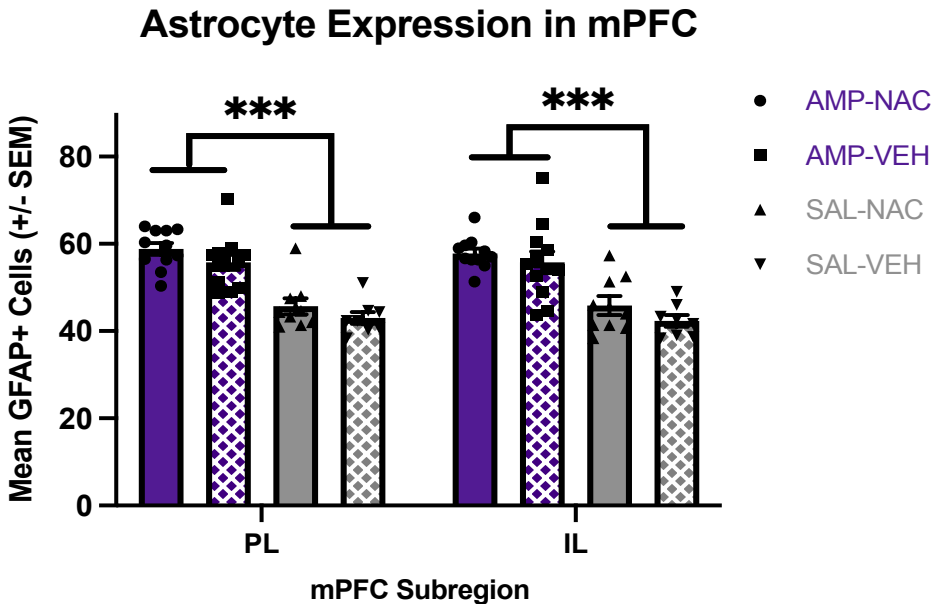

Figure 13. Mean (± SEM) GFAP expression within the PL and IL of the mPFC. Purple bars indicate animals that previously self-administered amphetamine (AMP) whereas grey bars indicate animals that previously self-administered saline (SAL). Solid bars indicate animals that received injections of N-acetylysteine (NAC) during abstinence and checkered bars denote animals that received injections of the saline vehicle (VEH). Bars and asterices indicate greater GFAP+ cell expression in amphetamine self-administering animals compared to saline, $p < .01$.

Table 6. *Results from Three-Way Analysis of Variance of Astrocyte Expression Within PL.*

	df	*SS*	*F*	*p*
Drug (AMP or SAL)	1	1669.02	62.06	**< .001**
Incubation Length (WD1 or WD14)	1	10.71	0.40	.53
Treatment (NAC or VEH)	1	76.89	2.86	.10
Incubation * Treatment	1	3.08	0.11	.74
Incubation * Drug	1	0.03	0.001	.98
Treatment * Drug	1	0.30	0.01	.92
Incubation * Treatment * Drug	1	34.68	1.29	.26
Error	33	887.56		
Total	40			

Note: Significance is indicated by boldfaced font

Table 7. *Results from Three-Way Analysis of Variance of Astrocyte Expression Within IL.*

	df	*SS*	*F*	*p*
Drug (AMP or SAL)	1	1569.92	39.09	**< .001**
Incubation Length (WD1 or WD14)	1	35.03	0.87	.36
Treatment (NAC or VEH)	1	56.81	1.41	.25
Incubation * Treatment	1	3.37	0.08	.77
Incubation * Drug	1	5.31	0.13	.72
Treatment * Drug	1	1.87	0.05	.83
Incubation * Treatment * Drug	1	14.09	0.35	.56
Error	33	1325.21		
Total	40			

Note: Significance is indicated by boldfaced font

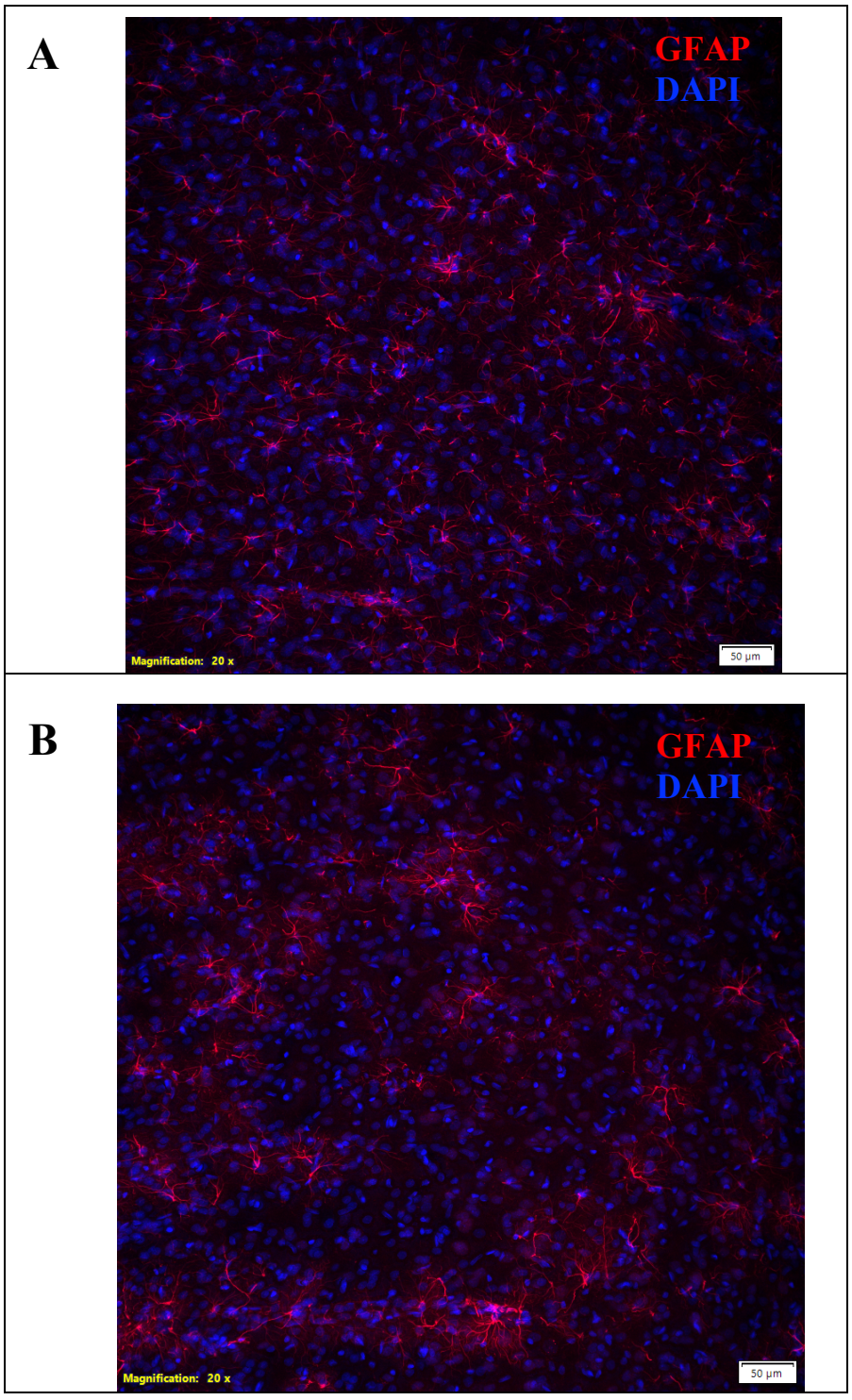

Figure 14. Representative 20X images of GFAP (astrocyte) and DAPI colocalization in the prelimbic cortex. (A) Representative image showing high GFAP expression, as quantified by cells showing both GFAP and DAPI expression. (B) Representative image showing low GFAP expression.

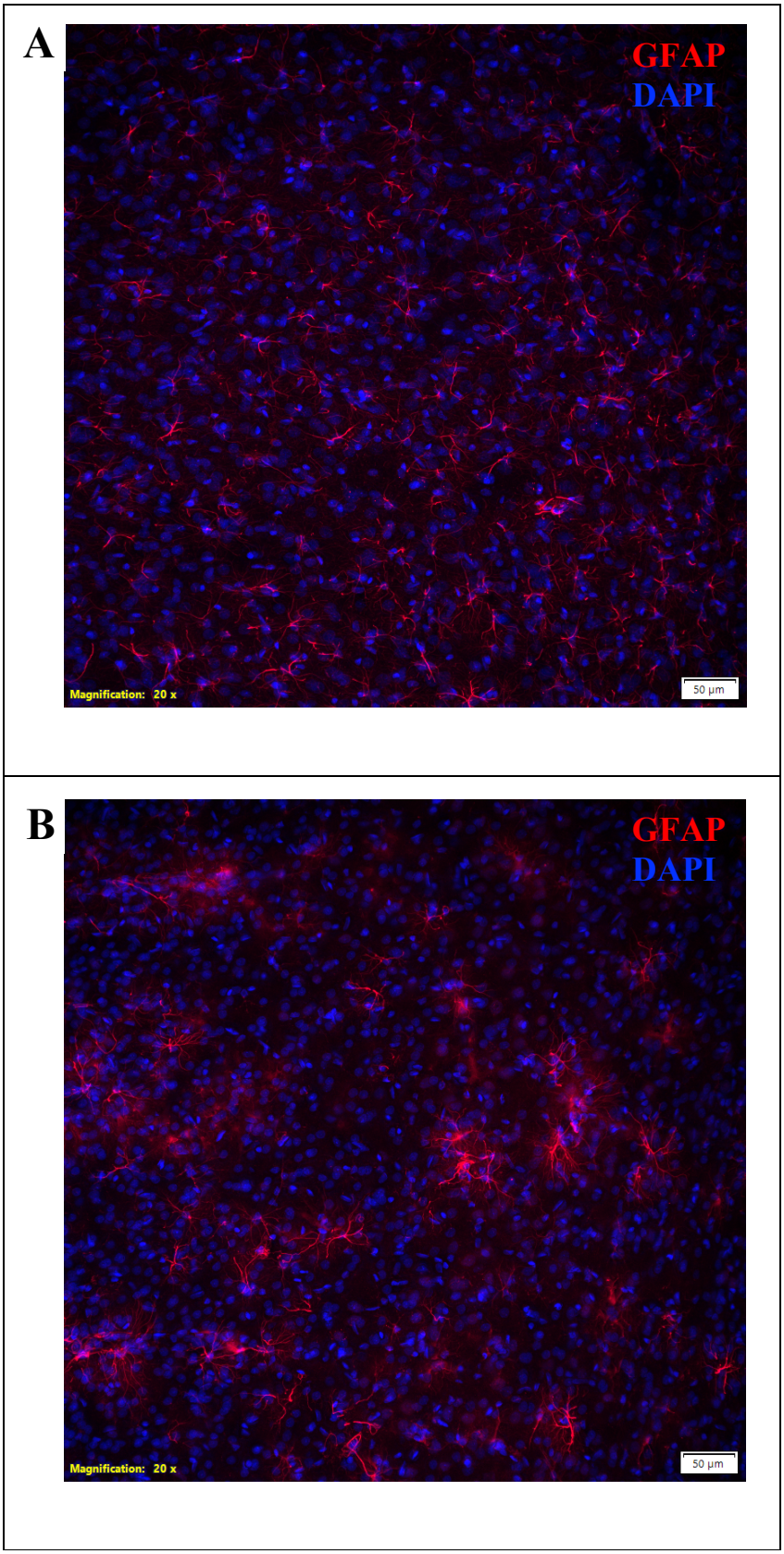

Figure 15. Representative 20X images of GFAP (astrocyte) and DAPI colocalization in the infralimbic cortex. (A) Representative image showing high GFAP expression, as quantified by cells showing both GFAP and DAPI expression. (B) Representative image showing low GFAP expression.

xCT Expression Within the Nucleus Accumbens

Two separate three-way ANOVAs were used to analyze xCT intensity within the ACb core and shell. Within the ACb core, there was a significant three-way interaction between Incubation length (WD1 or WD14), Treatment (NAC or VEH), and Self-Administration Drug Condition (Amphetamine or Saline), $F(1, 33) = 6.56$, $p = .01$. This effect was probed using a Tukey's HSD post-hoc test, which indicated that no significant differences in any condition. Within the ACb shell, the same three-way interaction was evident, $F(1, 33) = 8.08$, $p = .008$. Post-hoc analysis (Tukey's HSD) indicated several significant group differences within this three-interaction. Results of ANOVAs for both the ACb core and shell can be seen in Tables 8 and 9. Complete comparison matrices for both post-hoc tests are shown in Tables 10 and 11. Figures 16 and 17 show these effects for the ACb core and shell, respectively. Figures 18 and 19 show representative 20X micrographs of xCT within the ACb core and shell, respectively.

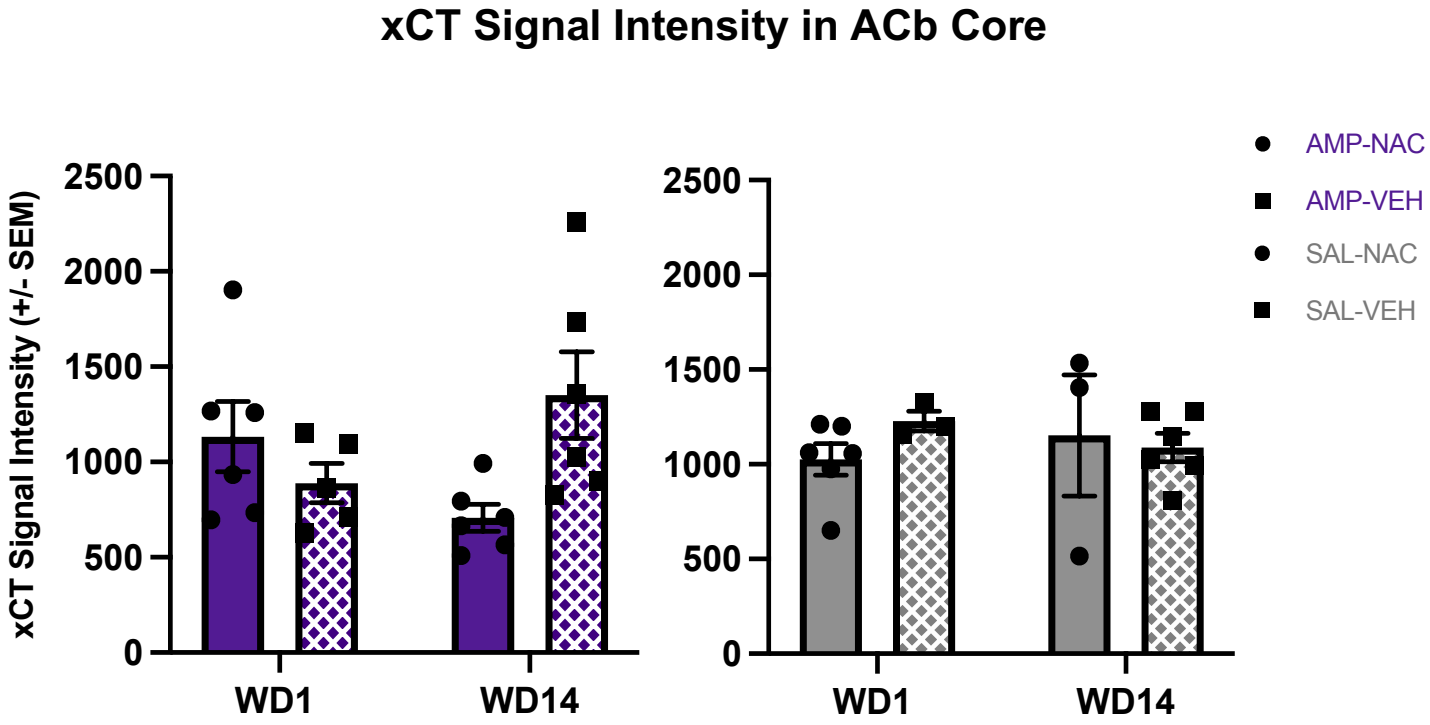

Figure 16. Mean (± SEM) xCT signal intensity within the ACb core. Purple bars indicate animals that previously self-administered amphetamine (AMP) whereas grey bars indicate animals that previously self-administered saline (SAL). Solid bars indicate animals that received injections of N-acetylysteine (NAC) during abstinence and checkered bars denote animals that received injections of the saline vehicle (VEH). Post-hoc probing of the significant three-way interaction (p = .01) did not indicate any significant pairwise comparisons.

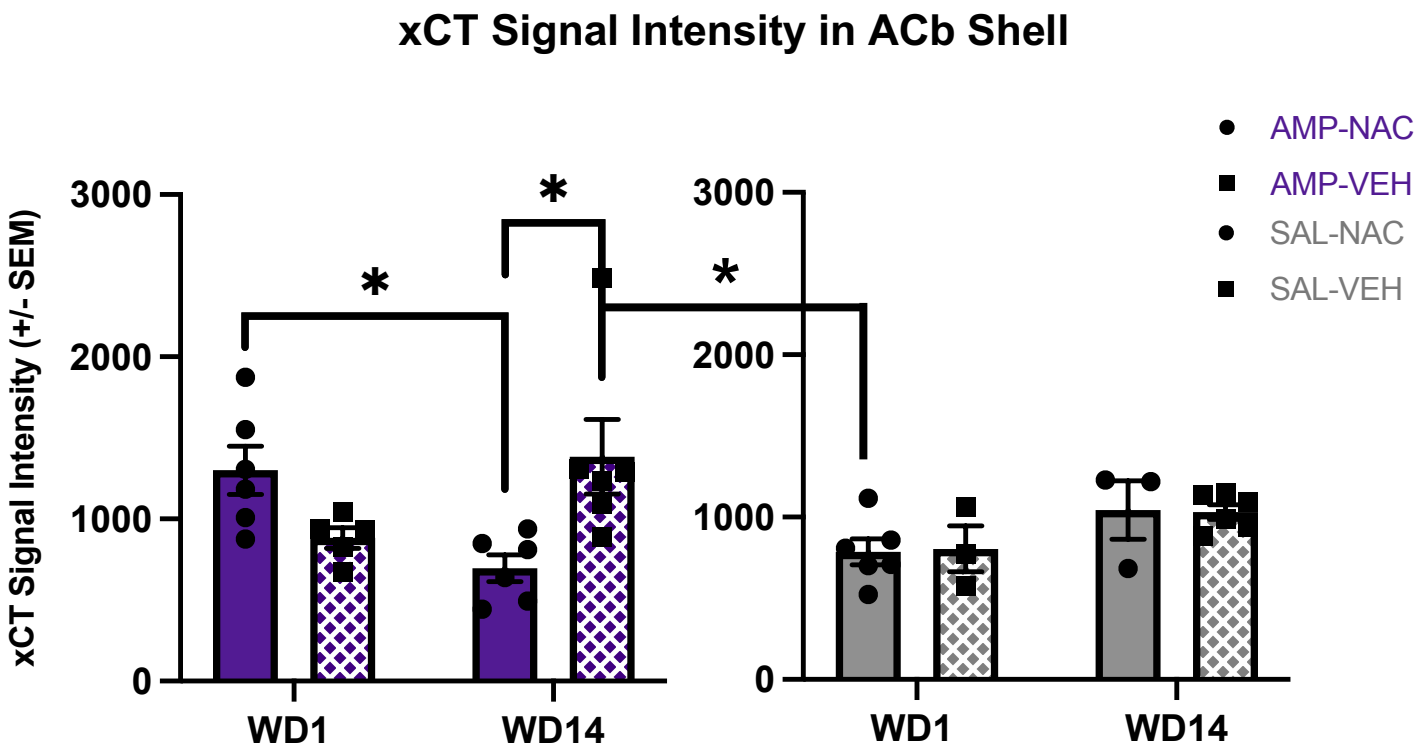

Figure 17. Mean (+/- SEM) xCT signal intensity within the ACb shell. Purple bars indicate animals that previously self-administered amphetamine (AMP) whereas grey bars indicate animals that previously self-administered saline (SAL). Solid bars indicate animals that received injections of N-acetylysteine (NAC) during abstinence and checkered bars denote animals that received injections of the saline vehicle (VEH) The bar and asterisk indicates a significant decrease in xCT signal intensity, $p < .01$.

Table 8. *Results from Three-Way Analysis of Variance of xCT Expression in the ACb Core*

	df	*SS*	*F*	*p*
Drug (AMP or SAL)	1	101870.85	0.85	.36
Incubation Length (WD1 or WD14)	1	258.45	0.002	.96
Treatment (NAC or VEH)	1	170801.64	1.43	.24
Incubation * Treatment	1	227277.36	1.90	.18
Incubation * Drug	1	1422.47	0.01	.91
Treatment * Drug	1	40440.63	0.34	.56
Incubation * Treatment * Drug	1	783770.61	6.56	**.02**
Error	33	3940991.6		
Total	40	5498136.9		

Note: Significance is indicated by boldfaced font

Table 9. *Results from Three-Way Analysis of Variance of xCT Expression in the ACb Shell*

	df	*SS*	*F*	*p*
Drug (AMP or SAL)	1	209761.23	2.23	.15
Incubation Length (WD1 or WD14)	1	85138.99	0.90	.35
Treatment (NAC or VEH)	1	44812.30	0.48	.50
Incubation Length * Treatment	1	678713.96	7.20	**.01**
Incubation Length* Drug	1	202239.78	2.15	.15
Treatment * Drug	1	41587.11	0.44	.51
Incubation Length * Treatment * Drug	1	761846.37	8.08	**.008**
Error	33	3110267.5		
Total	40	5560477.1		

Note: Significance is indicated by boldfaced font

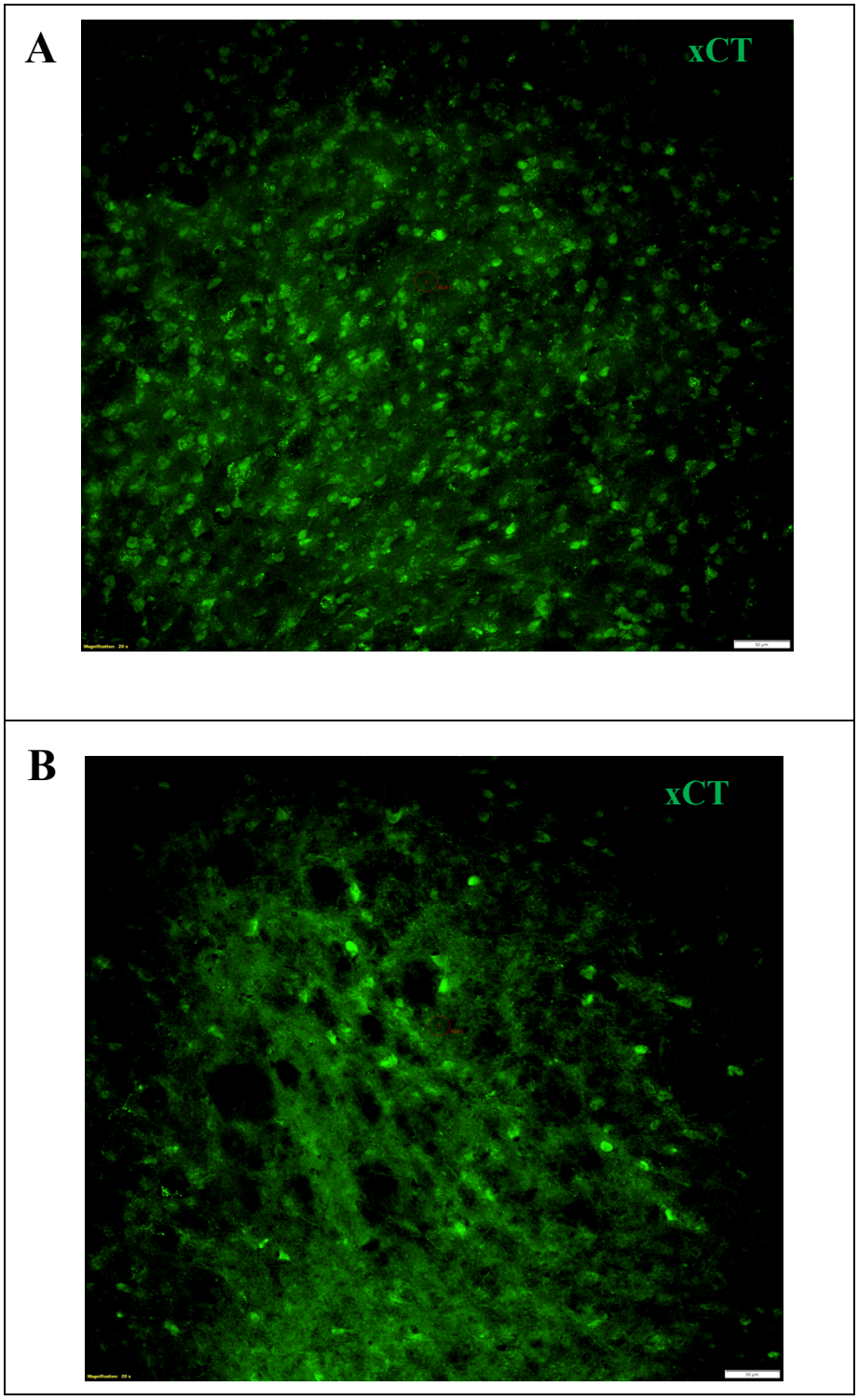

Figure 18. Representative 20X images of xCT expression in the ACb core. (A) Representative image showing high xCT expression. (B) Representative image showing low xCT expression.

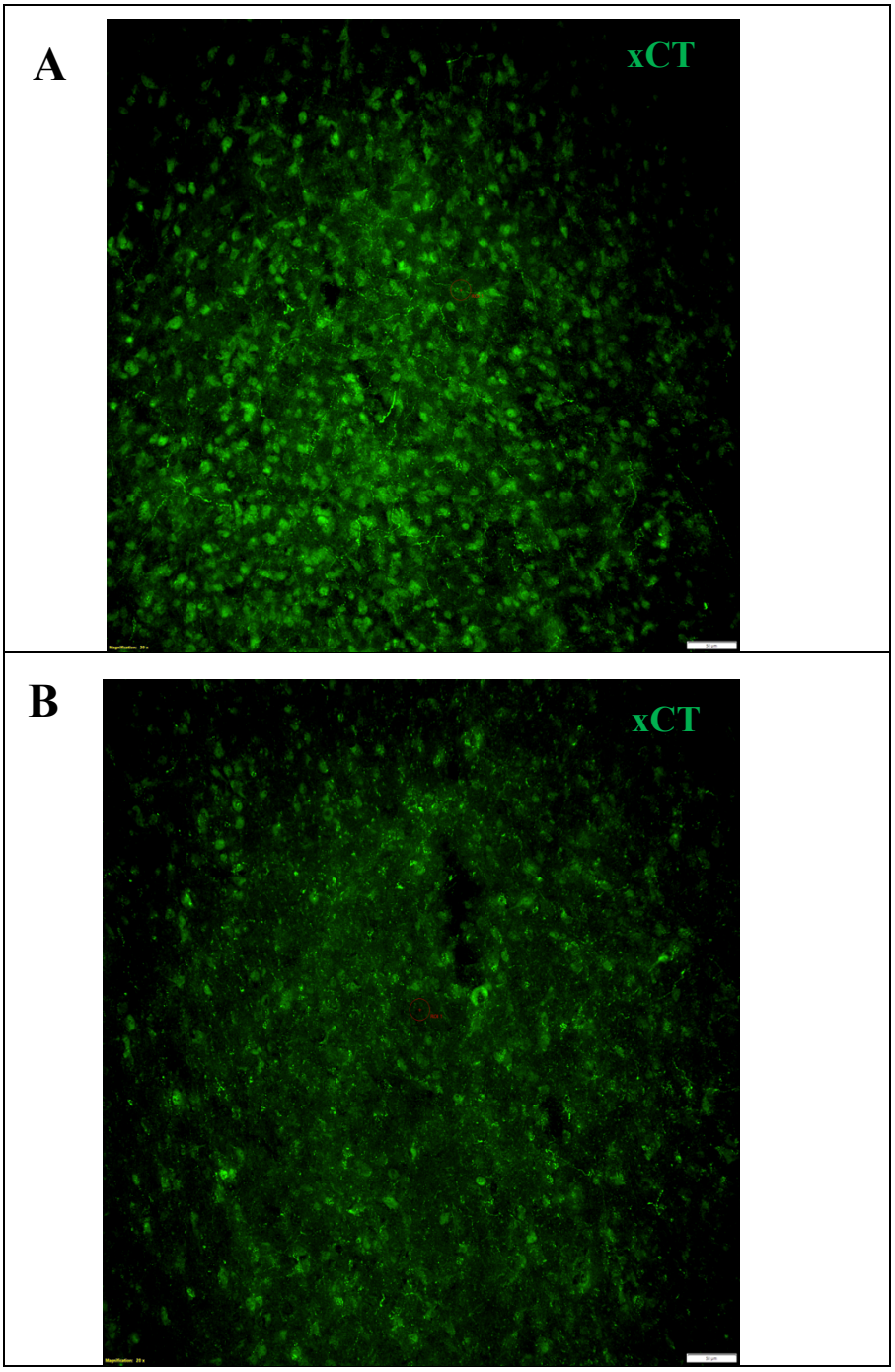

Figure 19. Representative 20X images of xCT expression in the ACb shell. (A) Representative image showing high xCT expression. (B) Representative image showing low xCT expression.

Table 10. *Results of Tukey's HSD post-hoc test for xCT expression within the ACb core.*

Mean[i]-Mean[j] Std Err Dif Lower CL Dif Upper CL Dif	Long,AMP, NAC	Long,AMP, VEH	Long,SAL, NAC	Long,SAL, VEH	Short,AMP, NAC	Short,AMP, VEH	Short,SAL, NAC	Short,SAL, VEH
Long,AMP,NAC	0	-644.24	-445.87	-381.85	-426.44	-182.73	-319.74	-522.09
	0	199.519	244.36	199.519	199.519	209.258	199.519	244.36
	0	-1289.2	-1235.8	-1026.9	-1071.4	-859.21	-964.75	-1312
	0	0.76738	344.095	263.149	218.565	493.755	325.259	267.878
Long,AMP,VEH	644.236	0	198.367	262.382	217.797	461.506	324.491	122.15
	199.519	0	244.36	199.519	199.519	209.258	199.519	244.36
	-0.7674	0	-591.6	-382.62	-427.21	-214.98	-320.51	-667.81
	1289.24	0	988.331	907.385	862.8	1137.99	969.494	912.114
Long,SAL,NAC	445.869	-198.37	0	64.015	19.4308	263.14	126.125	-76.217
	244.36	244.36	0	244.36	244.36	252.374	244.36	282.163
	-344.1	-988.33	0	-725.95	-770.53	-552.73	-663.84	-988.39
	1235.83	591.597	0	853.979	809.395	1079.01	916.089	835.955
Long,SAL,VEH	381.854	-262.38	-64.015	0	-44.584	199.125	62.1097	-140.23
	199.519	199.519	244.36	0	199.519	209.258	199.519	244.36
	-263.15	-907.38	-853.98	0	-689.59	-477.36	-582.89	-930.2
	1026.86	382.621	725.949	0	600.419	875.609	707.113	649.732
Short,AMP,NAC	426.438	-217.8	-19.431	44.5842	0	243.709	106.694	-95.648
	199.519	199.519	244.36	199.519	0	209.258	199.519	244.36
	-218.56	-862.8	-809.39	-600.42	0	-432.78	-538.31	-885.61
	1071.44	427.205	770.533	689.587	0	920.194	751.697	694.317
Short,AMP,VEH	182.729	-461.51	-263.14	-199.12	-243.71	0	-137.01	-339.36
	209.258	209.258	252.374	209.258	209.258	0	209.258	252.374
	-493.76	-1138	-1079	-875.61	-920.19	0	-813.5	-1155.2
	859.214	214.979	552.732	477.36	432.776	0	539.47	476.515
Short,SAL,NAC	319.744	-324.49	-126.12	-62.11	-106.69	137.015	0	-202.34
	199.519	199.519	244.36	199.519	199.519	209.258	0	244.36
	-325.26	-969.49	-916.09	-707.11	-751.7	-539.47	0	-992.31
	964.747	320.512	663.839	582.893	538.309	813.5	0	587.623
Short,SAL,VEH	522.086	-122.15	76.2167	140.232	95.6475	339.356	202.341	0
	244.36	244.36	282.163	244.36	244.36	252.374	244.36	0
	-267.88	-912.11	-835.96	-649.73	-694.32	-476.52	-587.62	0
	1312.05	667.814	988.389	930.196	885.612	1155.23	992.305	0

Significance is indicated in boldfaced font. No pairwise comparisons were significant at $\alpha = .05$.

Table 11. *Results of Tukey's HSD for xCT Expression in the ACb Shell.*

Mean[i]-Mean[j] Std Err Dif Lower CL Dif Upper CL Dif	Long,AMP, NAC	Long,AMP, VEH	Long,SAL, NAC	Long,SAL, VEH	Short,AMP, NAC	Short,AMP, VEH	Short,SAL, NAC	Short,SAL, VEH
Long,AMP,NAC	0	**-688.52**	-348.28	-334.84	**-604.53**	-186.95	-90.613	-109.11
	0	**177.248**	217.084	177.248	**177.248**	185.899	177.248	217.084
	0	**-1261.5**	-1050.1	-907.84	**-1177.5**	-787.92	-663.62	-810.9
	0	**-115.52**	353.502	238.164	**-31.523**	414.02	482.391	592.671
Long,AMP,VEH	**688.525**	0	340.242	353.684	83.9978	501.573	**597.912**	579.411
	177.248	0	217.084	177.248	177.248	185.899	**177.248**	217.084
	115.521	0	-361.54	-219.32	-489.01	-99.399	**24.9077**	-122.37
	1261.53	0	1042.03	926.688	657.002	1102.54	**1170.92**	1281.2
Long,SAL,NAC	348.282	-340.24	0	13.4417	-256.24	161.33	257.669	239.169
	217.084	217.084	0	217.084	217.084	224.203	217.084	250.666
	-353.5	-1042	0	-688.34	-958.03	-563.47	-444.11	-571.18
	1050.07	361.541	0	715.226	445.539	886.129	959.453	1049.52
Long,SAL,VEH	334.841	-353.68	-13.442	0	-269.69	147.888	244.228	225.727
	177.248	177.248	217.084	0	177.248	185.899	177.248	217.084
	-238.16	-926.69	-715.23	0	-842.69	-453.08	-328.78	-476.06
	907.845	219.32	688.342	0	303.318	748.86	817.232	927.511
Short,AMP,NAC	**604.527**	-83.998	256.245	269.686	0	417.575	513.914	495.414
	177.248	177.248	217.084	177.248	0	185.899	177.248	217.084
	31.5227	-657	-445.54	-303.32	0	-183.4	-59.09	-206.37
	1177.53	489.006	958.029	842.691	0	1018.55	1086.92	1197.2
Short,AMP,VEH	186.952	-501.57	-161.33	-147.89	-417.57	0	96.3394	77.8389
	185.899	185.899	224.203	185.899	185.899	0	185.899	224.203
	-414.02	-1102.5	-886.13	-748.86	-1018.5	0	-504.63	-646.96
	787.924	99.3994	563.469	453.084	183.397	0	697.311	802.638
Short,SAL,NAC	90.6128	**-597.91**	-257.67	-244.23	-513.91	-96.339	0	-18.501
	177.248	**177.248**	217.084	177.248	177.248	185.899	0	217.084
	-482.39	**-1170.9**	-959.45	-817.23	-1086.9	-697.31	0	-720.28
	663.617	**-24.908**	444.115	328.776	59.09	504.632	0	683.283
Short,SAL,VEH	109.113	-579.41	-239.17	-225.73	-495.41	-77.839	18.5006	0
	217.084	217.084	250.666	217.084	217.084	224.203	217.084	0
	-592.67	-1281.2	-1049.5	-927.51	-1197.2	-802.64	-683.28	0
	810.897	122.373	571.181	476.057	206.37	646.96	720.285	0

Significance is indicated in boldfaced font and indicates that $p < .05$.

xCT Expression Within the Medial Prefrontal Cortex

Two separate three-way ANOVAs were used to analyze xCT intensity within the PL and IL cortices. Within the PL, there was a significant three-way interaction between Incubation Length (WD1 or WD14), Treatment (NAC or VEH), and Drug Self-Administration condition (Ampethamine or Saline), $F(1, 36) = 7.27$, $p = .01$. Post-hoc probing of this interaction using Tukey's HSD test indicated one significant comparison. Namely, the mean difference between WD14-AMP-NAC and WD1-SAL-VEH groups was found to be statistically significant. Results of ANOVAs for both the PL and IL can be seen in Tables 12 and 13, respectively. A complete comparison matrix for this post-hoc test is shown in Table 14. Within the IL, results indicated a significant main effect of Treatment (NAC or VEH), such that NAC treatment was shown to decrease average xCT expression in IL, when collapsed across other experimental conditions, $F(1, 36) = 6.67$, $p = .01$. Additionally, the three-way interaction between Incubation Length (WD1 or WD14), Treatment (NAC or VEH), and Drug Self-Administration condition (Ampethamine or Saline), was found to be marginally significant, $F(1, 36) = 3.51$, $p = .06$. Given that this effect did not reach the *a priori* significance level of $\alpha = .05$, no further probing of this interaction was conducted. Figures 20 and 21 show these effects graphically. Figures 22 and 23 show representative 20X micrographs of xCT expression within the PL and IL, respectively.

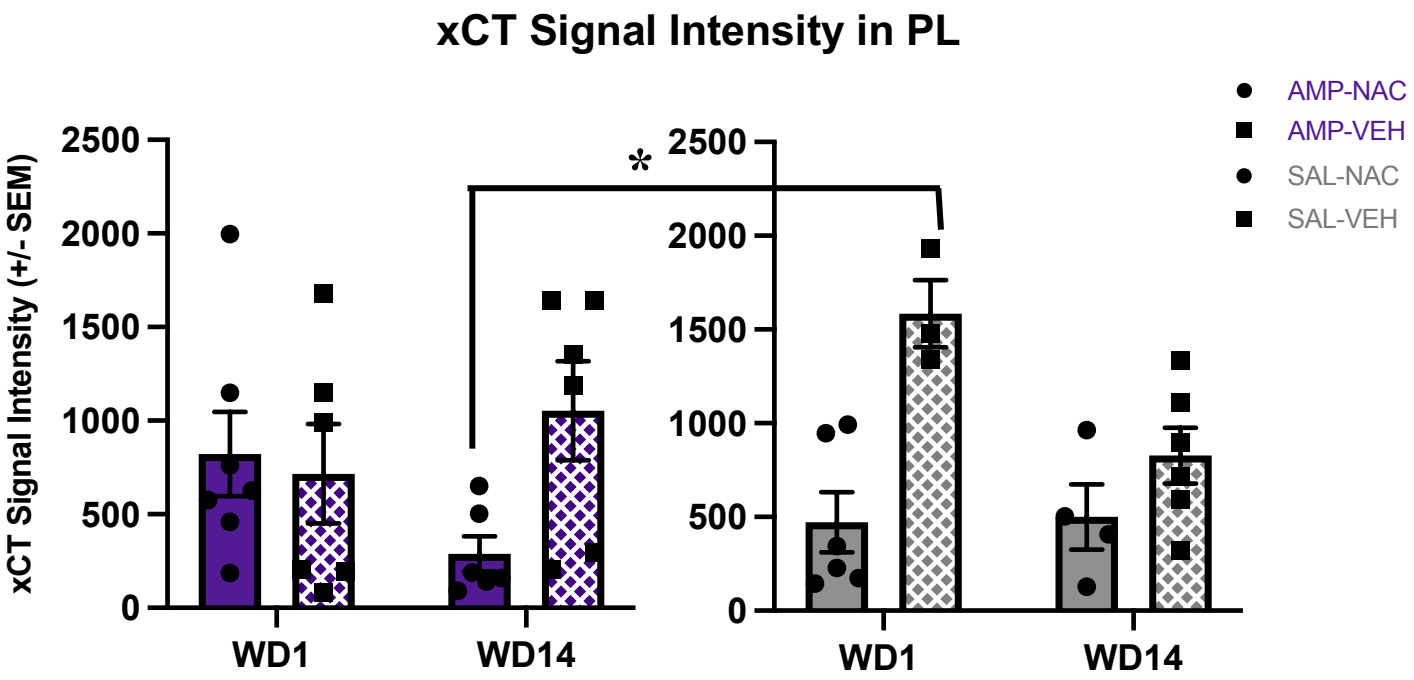

Figure 20. Mean xCT signal intensity (+/- SEM) within PL. Purple bars indicate animals that previously self-administered amphetamine (AMP) whereas grey bars indicate animals that previously self-administered saline (SAL). Solid bars indicate animals that received injections of N-acetylysteine (NAC) during abstinence and checkered bars denote animals that received injections of the saline vehicle (VEH). Lines and astuces indicate a significant pairwise comparison, $p < .05$.

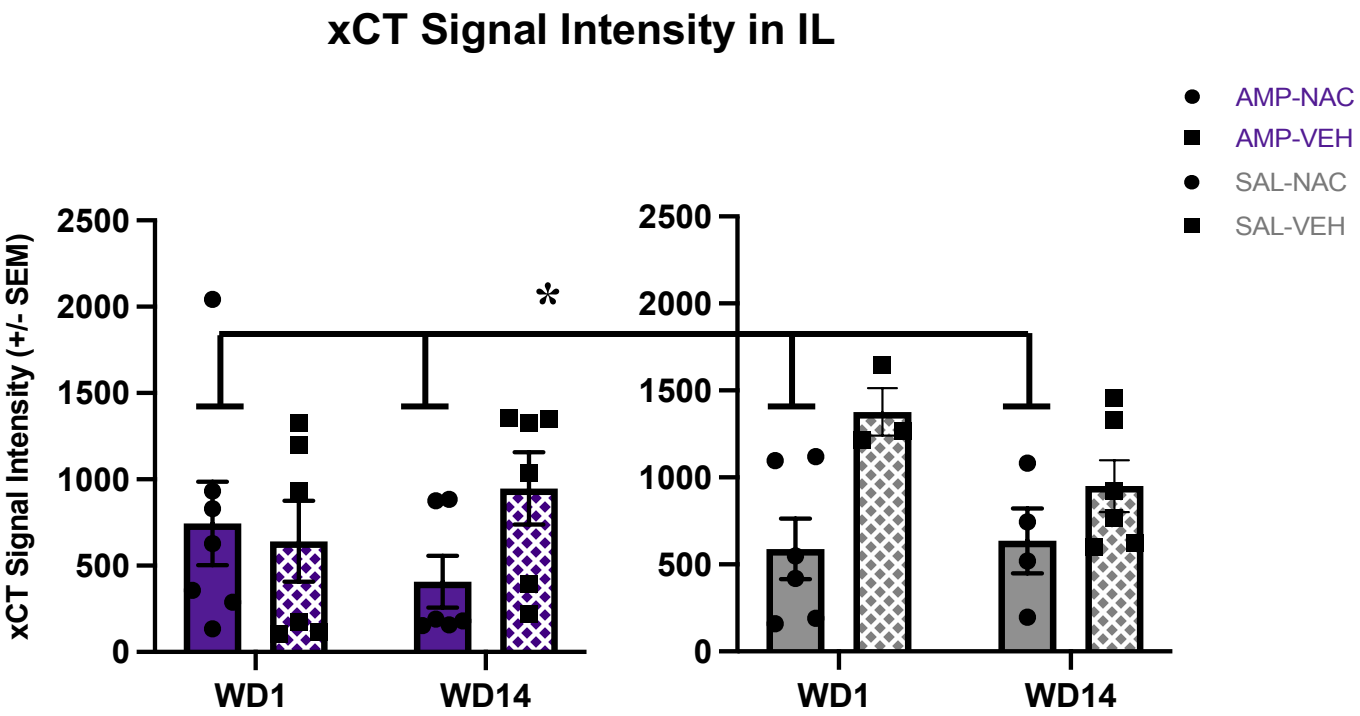

Figure 21. Mean xCT signal intensity (+/- SEM) within IL. Purple bars indicate animals that previously self-administered amphetamine (AMP) whereas grey bars indicate animals that previously self-administered saline (SAL). Solid bars indicate animals that received injections of N-acetylysteine (NAC) during abstinence and checkered bars denote animals that received injections of the saline vehicle (VEH). Asterices and bars indicate that average xCT intensity was significantly lower in NAC-treated animals when compared to VEH-treated animals, $p = .01$.

Table 12. *Results from Three-Way Analysis of Variance of xCT Expression in the PL.*

	df	*SS*	*F*	*p*
Drug (AMP or SAL)	1	167,840.8	0.70	.41
Incubation Length (WD1 or WD14)	1	558,601.5	2.34	.13
Treatment (NAC or VEH)	1	2,796,400.6	11.73	**.002**
Incubation Length * Treatment	1	5903.2	0.02	.88
Incubation Length* Drug	1	187883.9	0.79	.38
Treatment * Drug	1	380664.0	1.60	.21
Incubation Length * Treatment * Drug	1	1733330.5	7.27	**.01**
Error	36	8584509		
Total	43	13255261		

Note: Significance is indicated by boldfaced font

Table 13. *Results from Three-Way Analysis of Variance of xCT Expression in the IL.*

	df	*SS*	*F*	*p*
Drug (AMP or SAL)	1	421103.4	1.85	.18
Incubation Length (WD1 or WD14)	1	108400.2	0.48	.49
Treatment (NAC or VEH)	1	1519673.7	6.67	**.01**
Incubation Length * Treatment	1	18596.4	0.08	.78
Incubation Length* Drug	1	77852.6	0.34	.56
Treatment * Drug	1	283802.7	1.24	.27
Incubation Length * Treatment * Drug	1	799290.9	3.51	.06
Error	36	8208201		
Total	43	10844275		

Note: Significance is indicated by boldfaced font

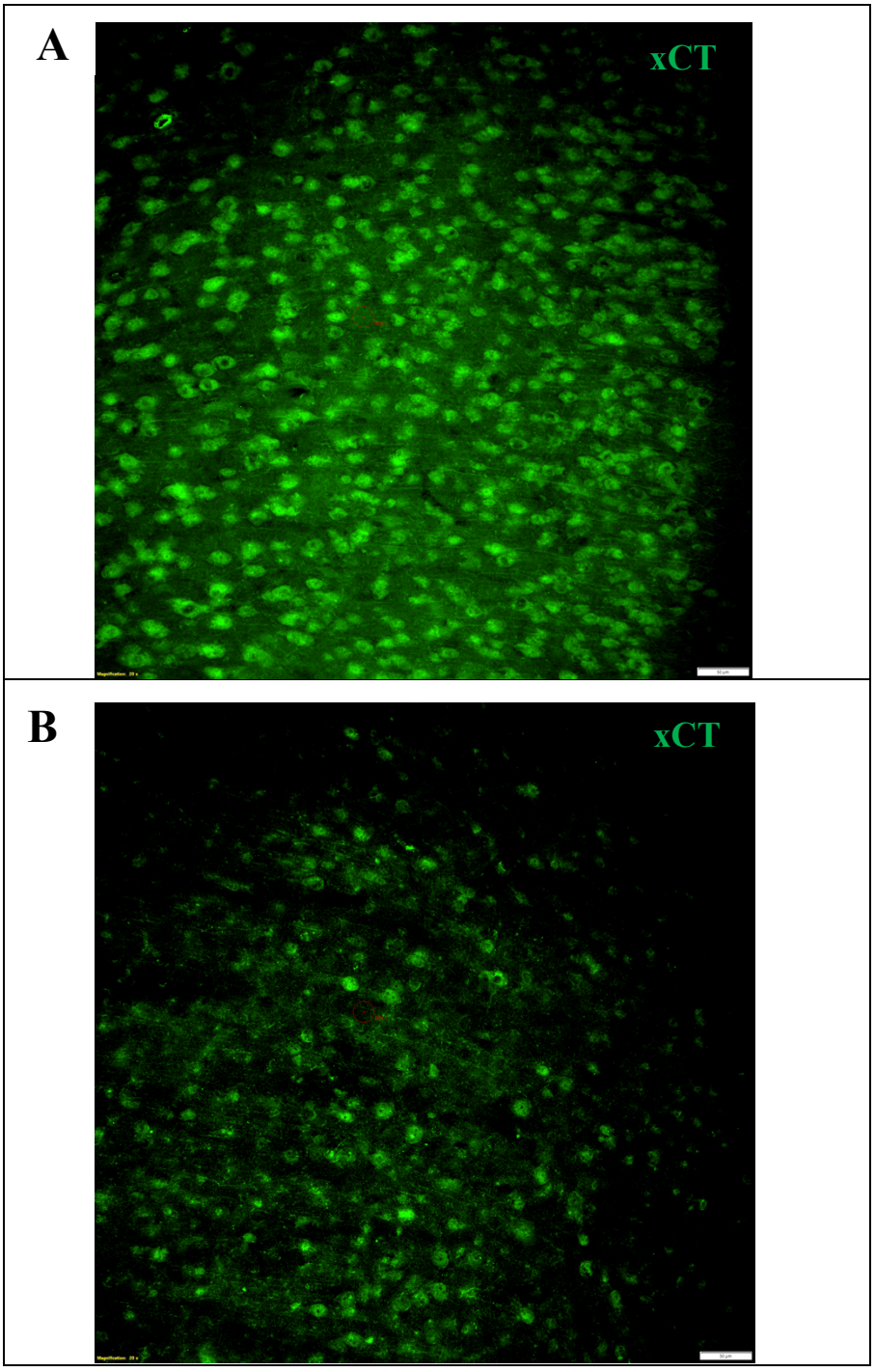

Figure 22. Representative 20X images of xCT expression in the PL cortex. (A) Representative image showing high xCT expression. (B) Representative image showing low xCT expression.

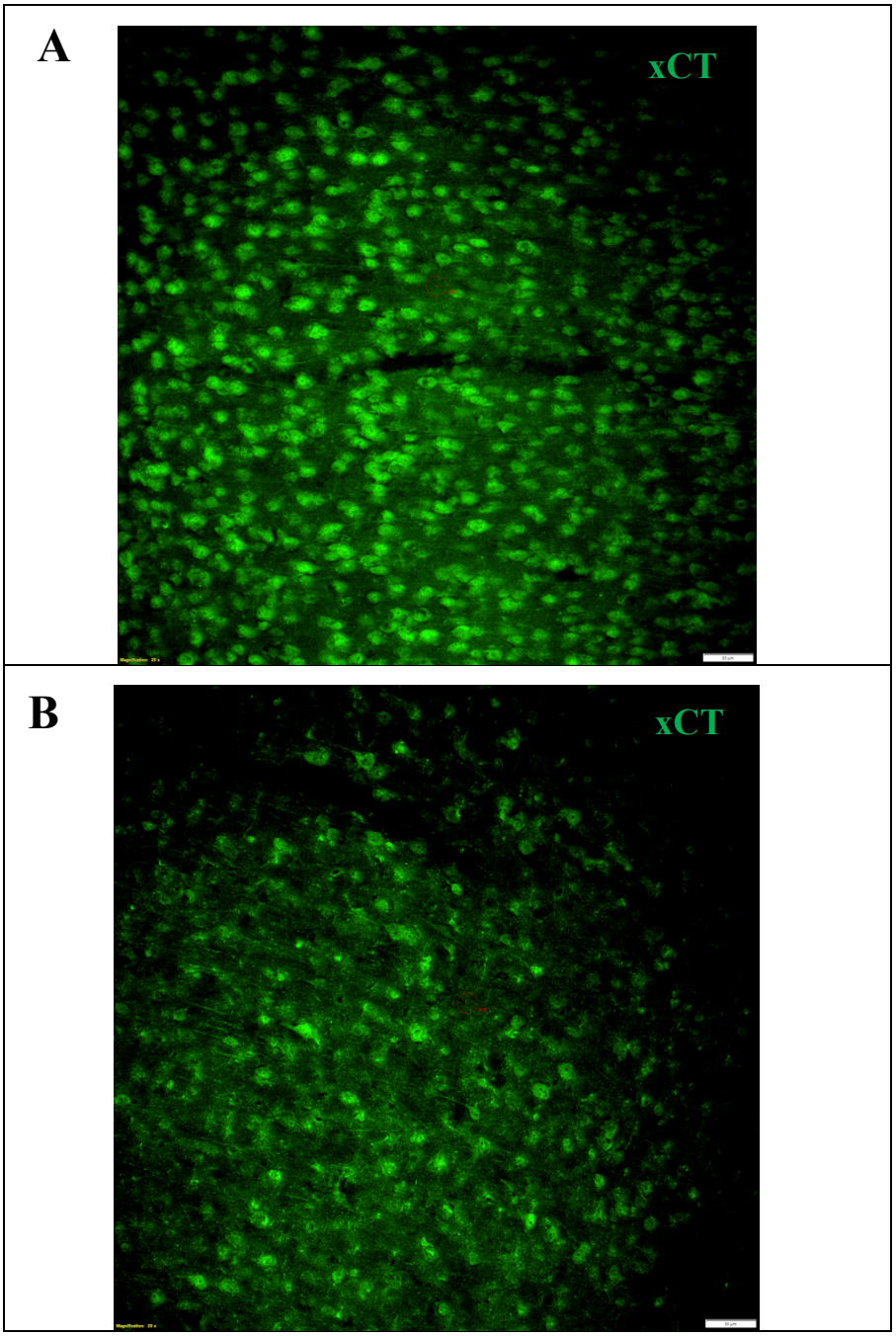

Figure 23. Representative 20X images of xCT expression in the IL cortex. (A) Representative image showing high xCT expression. (B) Representative image showing low xCT expression.

Table 14. *Results of Tukey's HSD Test for differences in xCT intensity in the PL cortex.*

Mean[i]-Mean[j] Std Err Dif Lower CL Dif Upper CL Dif	Long,AMP,NAC	Long,AMP,VEH	Long,SAL,NAC	Long,SAL,VEH	Short,AMP,NAC	Short,AMP,VEH	Short,SAL,NAC	Short,SAL,VEH
Long,AMP,NAC	0	-764.48	-210.99	-538.64	-533.03	-427.47	-192.61	**-1294.4**
	0	281.933	315.211	281.933	271.677	281.933	281.933	**345.296**
	0	-1671	-1224.5	-1445.2	-1406.6	-1334	-1099.2	**-2404.6**
	0	142.068	802.558	367.9	340.534	479.075	713.936	**-184.07**
Long,AMP,VEH	764.476	0	553.487	225.832	231.443	337.007	571.868	-529.88
	281.933	0	315.211	281.933	271.677	281.933	281.933	345.296
	-142.07	0	-460.06	-680.71	-642.12	-569.54	-334.68	-1640.2
	1671.02	0	1567.03	1132.38	1105.01	1243.55	1478.41	580.406
Long,SAL,NAC	210.989	-553.49	0	-327.66	-322.04	-216.48	18.3811	-1083.4
	315.211	315.211	0	315.211	306.072	315.211	315.211	372.962
	-802.56	-1567	0	-1341.2	-1306.2	-1230	-995.17	-2282.6
	1224.54	460.059	0	685.892	662.118	797.067	1031.93	115.879
Long,SAL,VEH	538.644	-225.83	327.655	0	5.61071	111.175	346.036	-755.71
	281.933	281.933	315.211	0	271.677	281.933	281.933	345.296
	-367.9	-1132.4	-685.89	0	-867.96	-795.37	-560.51	-1866
	1445.19	680.711	1341.2	0	879.178	1017.72	1252.58	354.574
Short,AMP,NAC	533.033	-231.44	322.044	-5.6107	0	105.564	340.425	-761.32
	271.677	271.677	306.072	271.677	0	271.677	271.677	336.974
	-340.53	-1105	-662.12	-879.18	0	-768	-533.14	-1844.8
	1406.6	642.124	1306.21	867.957	0	979.132	1213.99	322.206
Short,AMP,VEH	427.469	-337.01	216.48	-111.17	-105.56	0	234.861	-866.89
	281.933	281.933	315.211	281.933	271.677	0	281.933	345.296
	-479.07	-1243.6	-797.07	-1017.7	-979.13	0	-671.68	-1977.2
	1334.01	569.536	1230.03	795.369	768.003	0	1141.4	243.399
Short,SAL,NAC	192.608	-571.87	-18.381	-346.04	-340.43	-234.86	0	-1101.7
	281.933	281.933	315.211	281.933	271.677	281.933	0	345.296
	-713.94	-1478.4	-1031.9	-1252.6	-1214	-1141.4	0	-2212
	1099.15	334.675	995.165	560.508	533.142	671.683	0	8.53799
Short,SAL,VEH	**1294.35**	529.878	1083.37	755.711	761.321	866.886	1101.75	0
	345.296	345.296	372.962	345.296	336.974	345.296	345.296	0
	184.07	-580.41	-115.88	-354.57	-322.21	-243.4	-8.538	0
	2404.64	1640.16	2282.61	1866	1844.85	1977.17	2212.03	0

Significance is indicated in boldfaced font and indicates that $p < .05$.

Chapter 5 - Discussion

Summary of Main Results

The current study offers several key insights which help to fill voids in the understanding of the treatment and neurobiology of cue-induced relapse to amphetamine. First, our data show that incubation of drug craving did not occur following short-access amphetamine self-administration. Second, the therapeutic NAC is not effective in attenuating cue-induced relapse during acute or protracted abstinence from amphetamine-use. Third, these data show that amphetamine significantly increases astrocyte expression within both regions of the mPFC and ACb. Finally, these data suggest that repeated NAC treatment during the abstinence period can actually decrease xCT expression within both the mPFC and ACb. Together, these findings suggest that while NAC decreases xCT expression, it has limited effectiveness for the attenuation of cue-induced craving for amphetamine.

Potential Cohort Differences in Amphetamine Self-Administration

While the observation of cohort-specific differences in average amphetamine self-administration is unexpected, it's importance is undermined by several noteworthy factors. First, given the relatively small difference in the group means of Cohorts 1 and 2, this effect is plausibly driven from remarkably low variability present across amphetamine self-administering rats. Second, given that amphetamine and saline self-administering rats were counterbalanced across the four cohorts, some cohorts had larger group sizes than other cohorts (see the legend of Figures 7 and 8 for group sizes for each of the four cohorts). This may have impacted the variability within each cohort, plausibly affecting the significance or lack of significance in specific cohort comparisons.

It is common convention in the field of operant drug self-administration to test for cohort effects and confirm stable responding using the last several self-administration sessions (Arndt, Johns, Dietz & Cain, 2015; Garcia, Arndt & Cain, 2019; Shahbazi, Moffett, Williams & Frantz, 2008). Together, the small differences between Cohorts 1 and 2 across all self-administration sessions, and the lack of a cohort effect during the last 7 self-administration sessions, suggest that responding for amphetamine was approximately equivalent across the cohorts prior to the cue-test.

2-Hr Continuous Access to Amphetamine During Self-Administration Training

Overall, results from the self-administration portion of the current study indicate a reliable and robust preference for active-lever responding for amphetamine compared to saline, as predicted. Additionally, these self-administration results indicate that amphetamine self-administering rats showed distinct preference for responding to the active-lever over the inactive lever. Though we did show a robust preference for amphetamine over the saline vehicle during self-administration, we did not see significant escalation in amphetamine-intake across the 14 self-administration sessions utilized. This finding is in keeping with research suggesting that escalations in drug-intake predominately occur following extended-access drug self-administration (Ahmed and Koob, 1998).

Incubated Cue-Induced Craving Does Not Occur Following 2-Hr Continuous Access Self-Administration Sessions for Amphetamine

In the current study, it was predicted that the high dose of amphetamine utilized would be sufficient to produce incubation in drug craving from Withdrawal Day 1 to Withdrawal Day 14,

despite only being available in short-access self-administration sessions. However, the current study found that cue-induced amphetamine craving did not increase or incubate during the forced abstinence period. Succinctly, animals tested on Withdrawal Day 14 did not show higher levels of cue-induced craving when compared to those tested at Withdrawal Day 1 as predicted. This finding merits several points of discussion as it highlights potential voids in previous literature on the incubation of cue-induced craving for amphetamine.

There is a plethora of literature showing a reliable and robust increase in cue-induced craving following forced drug-abstinence across a number of different drugs of abuse. For instance, there is evidence illustrating incubation of craving for methamphetamine (Caprioli, Venniro, Zhang, Bosser, Warren, Hope, & Shaham, 2017; Li, et al., 2015;), cocaine (Grimm, et al., 2001; Mead, et al., 2007), heroin (Shalev, et al, 2001; Airavaara, et al., 2011), nicotine (Abdolahi, et al, 2010), and alcohol (Bienkowski, et al., 2004). However, a review of this literature suggests that the most robust incubation effects, regardless of drug or drug class, occur following extended-access self-administration models (i.e. 6-9 hrs of self-administration per session) (Wolf, 2016; Lu, Grimm, Hope, & Shaham, 2004). While short-access self-administration models (1 or 2 hrs of self-administration per session) can elicit increases in cue-induced drug-seeking during abstinence, these effects occur rather inconsistently and seem to be most prominent following short-access to cocaine (Swinford-Jackson, Anastasio, Fox, Stutz, & Cunningham, 2016).

Based on current understanding, incubation of cue-induced drug-craving has not be observed for amphetamine. One plausible conclusion for why incubation in cue-induced craving were not observed in the current study is that the timeline for the incubation of amphetamine craving requires a different abstinence period in order to see the effect. While increases in drug-

seeking for cocaine, heroin, nicotine, and methamphetamine are evident within 2-3 weeks of abstinence to the drug following long-access paradigms, it is possible that the increase in drug-seeking for amphetamine occurs on a much longer time scale. However, recent work from our lab has shown that short-access amphetamine self-administration (1 hour of access per session for 16 days) did not increase cue-induced amphetamine craving at Withdrawal Day 40 when compared to Withdrawal Day 1 (Garcia, & Cain, 2021). Given these data demonstrate that craving did not increase when tested on more protracted scale than the withdrawal periods tested in the current study (WD40 vs WD14), it is unlikely that the duration of abstinence is what accounted for the lack of an incubation effect from WD1 to WD14 in the present study.

Therefore, the most plausible conclusion is that long-access self-administration is required in order to elicit incubations in cue-induced craving for amphetamine. Evidence from both cocaine and methamphetamine self-administration supports this conclusion given that long, but not short-access, self-administration procedures result in accumulations of CP-AMPA receptors at excitatory synapses in the ACb core (Purgianto, Scheyer, Loweth, Ford, Tseng, & Wolf, 2013; Loweth, Tseng, & Wolf, 2014; Murray et al., 2019). This accumulation of CP-AMPA receptors ultimately drives long-term potentiation at glutmatergic synapses and the incubation of craving during the course of drug abstinence. Though there is little information regarding specific changes in CP-AMPA receptor expression following amphetamine self-administration and abstinence, a review of the literature suggests that increases in CP-AMPA receptor expression are more largely due to longer-access self-administration models than they are to different psychostimulants (e.g. methamphetamine, cocaine, etc.). Importantly, though increases in CP-AMPA receptor expression explain a mechanism for LTP of glutamatergic synapses and increased cue-induced craving, there are multiple more proximal issues that could

allow the same increase in CP-AMPA receptor expression to occur at the synapse. This hypothesis is supported by the fact that expression of both mGluR1/5 and mGluR2/3 are inversely related with CP-AMPA expression and that loss of glutamatergic tone on pre- or post-synaptic mGluRs precludes long-term depression (LTD) mechanisms and a concomitant increase in CP-AMPA receptor expression (Loweth, et al., 2019; Loweth, Scheyer, et al., 2014). At the onset of this study, it was theorized that the xCT to pre-synaptic mGluR2/3 LTD mechanism could be one such mechanism for mitigating the strengthening of glutamatergic synapses following amphetamine self-administration and abstinence. The plausibility of this theory will continue to be evaluated through subsequent sections of this thesis.

N-acetylcysteine (NAC) Does Not Attenuate Cue-Induced Amphetamine-Seeking During Acute or Protracted Withdrawal

The current study was designed to extend the existing literature showing NAC's efficacy to reduce relapse to amphetamine-associated cues. The methods utilized were consistent with work showing that NAC was effective in lowering cue induced drug-seeking for both methamphetamine and cocaine (Reichel et al., 2011; Siemsen et al., 2019). Given its efficacy for treating relapse to cocaine, we derived both our withdrawal period (14 days of abstinence to the drug) and NAC dose (100 mg/kg; ip) from studies showing NAC's potential efficacy in attenuating cue-induced relapse to cocaine (Reichel et al., 2011) and reinstatement to methamphetamine (Siemsen et al., 2019). With that being said, though both studies found that NAC (100 mg/kg; ip) was effective for lowering cue-induced cocaine relapse or methamphetamine reinstatement, this same dose is insufficient to lower cue-induced relapse to

amphetamine. It is possible that a different dose of NAC may be required to low cue-induced relapse to amphetamine.

It is important to note that the preponderance of studies showing NAC's efficacy in mitigating cue-induced drug-seeking across multiple drugs of abuse did not assess cue-induced craving at more than one relapse or reinstatement session during the abstinence period (Siemsen et al., 2019; Reichel et al., 2011). As such, we are confident that the efficacy of NAC is not contingent on incubations in craving during abstinence. Therefore, the lack of such an incubation effect in the current study does not present a reason why NAC failed to attenuate cue-induced drug craving at either WD 1 or WD 14.

The finding that NAC was ineffective at lowering cue-induced relapse during either acute or protracted withdrawal conditions is noteworthy and highlights important distinctions between therapeutic interventions for different drugs of abuse. Though NAC has been shown to be effective in lowering cue-induced relapse to cocaine (Reichel et al., 2011; Murray, Everitt, & Belin, 2012; Moussawi et al., 2009), the current study has shown that this efficacy does not extend to amphetamine. Additionally, the efficacy of NAC in mitigating cue-induced craving for methamphetamine has been inconsistently demonstrated in both preclinical and clinical models. For instance, while Siemsen et al. (2019) found that NAC was effective in lowering cue-induced reinstatement to methamphetamine, work from Charntikov et al. (2018) demonstrated that NAC was not able to attenuate cue-induced reinstatement to methamphetamine. This inconsistency is also evident in human clinical trials with one study showing a reduction in methamphetamine cravings following NAC treatment (Mousavi et al., 2015), but a comparable study showing no reduction in methamphetamine craving following NAC treatment (Grant et al., 2010). Overall, this review of the literature suggests that the efficacy of NAC treatment for methamphetamine is

likely inconsistent, at best. Taken together, these findings suggest that NAC's efficacy may be limited to certain psychostimulants (e.g. cocaine) but does not extend to other compounds within the same drug class (e.g. amphetamine and methamphetamine).

Though cocaine and amphetamine are both classified as psychostimulants, there are well-defined neurochemical distinctions and mechanisms of action. The primary mechanism mediating the abusive potential of psychostimulants is their ability to bind dopamine transporters (DAT) (Seiden, Sabol, & Ricurarte, 1993; Ritz, Lamb, Goldberg, & Kuhar, 1987). However, the mechanism by which dopamine is eliminated and trafficked from the synaptic, and extrasynaptic areas, differs between amphetamine and cocaine. While cocaine is able to bind directly to DAT, it is not able to be transported into the presynaptic neuron. Therefore, cocaine is not able to effectively replace the action of dopamine (White, Watchel, Johansen, & Einhorn, 1987). Conversely, amphetamine also directly binds to DAT and is also able to be trafficked back into the presynaptic neuron. Here, the alkaline pH of amphetamine is able to degrade dopamine vesicles which results in accumulations of dopamine within the cellular cytosol (Sulzer, Maidment, & Rayport, 1993). In short, while both amphetamine and cocaine interact with DAT to increase dopamine levels, they accomplish this via different mechanisms (Kalivas, 2007).

In addition to it's differences to cocaine, there are well characterized distinctions between the neurobiological mechanisms implicated in methamphetamine and amphetamine exposure. Using in vivo microdialysates, Shoblock et al. (2003) determined that there amphetamine and methamphetamine exposure produce separable effects on dopamine and glutamate release within the mPFC and ACb. Specifically, while both amphetamine and methamphetamine increase dopamine levels within mPFC, amphetamine produces a larger increase in extracellular dopamine when compared to those produced by methamphetamine. Within the ACb,

amphetamine was shown to increase glutamate levels while methamphetamine was not. This effect on glutamate release was reversed in the mPFC with methamphetamine increasing glutmate levels while amphetamine failed to do so. It is entirely possible that the differences in these mechanisms could result in differences in the efficacy of NAC for different psychostimulants.

Astrocyte Expression Within the Nucleus Accumbens and Medial Prefrontal Cortex is Altered by Amphetamine Exposure

The current study found that previous exposure to amphetamine during self-administration was associated with increases in the number of GFAP+ astrocytes within the ACb core and shell as well as both the prelimbic (PL) and infralimbic (IL) cortices of the medial prefrontal cortex (mPFC). This finding is in keeping with previous literature showing that exposure to psychostimulants can increase astrocyte expression (Bowers & Kalivas, 2003).

One potential explanation for why such an increase would occur is that this could serve as a compensatory mechanism for declining xCT expression on the surface of astrocytes. However, this increase could prove to be deleterious due to potential neuroinflammation that would occur with large increases in astrocyte expression. Neuroinflammation has been hypothesized to contribute to drug-induced neurotoxicity for a number of drugs of abuse (Kousik, Napier, & Carvey, 2012). Another alternative hypothesis for why astrocyte expression would increase following exposure to amphetamine is due to a potential increase in extracellular glutamate in response to amphetamine. These increases in glutamate may stimulate mGluR5 receptors, which are abundant on the surface of astrocytes. Activation of mGluR5 has been shown to increase astocyte [mehtl-^{3}H]thymidine incorporation (Ciccarelli et al., 1997). The

significance of the interaction between psychostimulants and the mGluR5 system is also ameliorated by the finding that mGluR5 gene deletion attenuates the rewarding and psychomotor effects of cocaine in mice (Chiamulera et al., 2001).

The Effect of Repeated NAC Treatment on xCT Expression is Moderated by Previous Exposure to Amphetamine and Abstinence Duration

The current study found a significant three-way interactions between Treatment (NAC or VEH), Drug Self-Administration condition (amphetamine or saline), and the Withdrawal Period (WD1 or WD14) within both the ACb and mPFC. In the ACb shell, this three-way interaction was evidenced by the finding that repeated NAC treatment decreased overall xCT expression at WD14 when compared to WD1 (see Figures 18 and 19), whereas repeated injections of the saline VEH treatment tended to increase overall xCT expression at WD14. One plausible explanation for an increase in xCT expression following repeated treatment with the saline VEH could be an overall increase in GFAP+ cell expression that was shown previously in response to amphetamine. Though the same three-way interaction was found to be statistically significant within the ACb core, post-hoc analysis did not indicate and significant pairwise comparisons. These null comparisons in the ACb core illustrate the greater variability that was present in xCT expression within the ACb core. It is entirely possible that the conservative post-hoc tests utilized coupled with the increased variability present, could have precluded significant effects despite a significant omnibus effect. Taken together, these data from the ACb suggest a link between repeated NAC treatment and xCT expression following exposure to amphetamine.

The same three-way interaction was found to be significant within the PL cortex. Though post-hoc testing only revealed one significant pairwise comparison (see Figure 20 and Tables 13

and 15), xCT expression within the PL followed similar trends to the ACb. Repeated NAC treatment tended to decrease xCT expression at WD14 for animals exposed to amphetamine while treatment with the saline-vehicle tended to increase xCT expression at WD14. Within the IL, the same three-way interaction was found to only be marginally significant ($p = .06$). Again, though significant comparisons were not indicated, trends for the IL cortex followed the same patterns present in the PL and ACb.

The effects of NAC treatment on xCT expression are of significant interest to the current study. Specifically, the finding that repeated NAC treatment decreased xCT expression in the ACb and mPFC are highly interesting given that xCT is the specific mechanism of action for NAC's efficacy in restoring glutamate homeostasis (Murray, Lacoste & Belin, 2014). NAC does so by supplying extracellular cysteine to stimulate xCT-mediated glutamate release. This increase in extracellular glutamate is sufficient to bind mGluR2/3 autoreceptors. mGluR2/3 autoreceptors regulate presynaptic glutamate release. Therefore, glutamate binding to mGluR2/3 should inhibit presynaptic glutamate release and concomitant neuronal potentiation in the ACb and mPFC (Moran et al., 2005; Moussawi et al., 2009).

The finding that xCT was to found to be disrupted within the ACb shell, and at least somewhat impaired in the IL cortex is noteworthy given the behavioral role of IL-ACb shell projection neurons during abstinence and relapse. While PL-ACb core projections are largely responsible for the execution of behavior, IL-ACb shell glutamatergic projections are vital for response inhibition (Gass & Chandler, 2013; Van den Oever et al., 2010). Pharmacological inactivation (e.g. muscimol, baclofen) of IL-ACb shell projections increases lever pressing and spontaneous recovery of extinguished cocaine self-administration following 28 days of forced abstinence (Peters et al., 2008). Given these findings, a decrease in xCT and disruption of

glutamate homeostasis within the ACb shell and IL could produce similar effects as those produced by inactivation of IL-ACb shell projections. As such, these disruptions in glutamate homeostasis within the ACb shell and IL could result in an inability to inhibit responding during relapse testing, thus producing a habitual pattern of cue-induced responding characteristic of addiction and chronic relapse.

A Molecular Basis for the Inefficacy of *N*-Acetylcysteine

Given that xCT-mediated glutamate release is the primary mechanism of action for NAC, the finding that repeated NAC treatment decreased xCT expression, when measured at WD 14, is quite surprising. This finding suggests that the xCT-mGluR2/3 system may not be implicated in amphetamine-use disorder and cue-induced relapse to amphetamine-seeking. To assess the plausibility of this conclusion, an exploratory analysis was conducted by limiting analysis to animals that received the saline vehicle treatment. The drug that was self-administered (amphetamine or saline), the withdrawal period (WD 1 or WD 14), and their interaction were included as predictors of xCT expression. Within the ACb shell, this analysis indicated that there was a significant main effect of incubation length, such that xCT expression was significantly higher at WD 14, $F(1, 16) = 5.29$, $p = .04$. However, neither the drug self-administration condition or the two-interaction between incubation length and drug self-administration condition were found to be significant. Neither main effect or their interaction were found to be significant in the ACb core or the IL and PL cortices. Taken together, these results suggest that xCT may not be the mechanism responsible for cue-induced relapse to amphetamine during drug abstinence. This conclusion is behaviorally corroborated by our finidngs showing that NAC was

ineffective at lowering cue-induced relapse, as the mechanism of action for NAC is not altered following exposure to amphetamine.

However, the question still remains as to why repeated NAC injections would decrease xCT expression at WD 14. Evidence from work with the supplement, L-cysteine, provides some viable conclusions regarding this finding. L-cysteine is remarkably similar to NAC with regard to its chemical structure, differing from NAC only in its lack of N-acetyl group. However, it's pharmacological similarity is even more evident given that NAC is cysteine-prodrug which serves as a precursor molecule for L-cysteine and glutathione (Murray, Everitt, & Belin, 2012). As such, NAC and L-cysteine have remarkable chemical and pharmacological similarity. Additionally, the role of L-cysteine in neuromodulation is well documented (Keller, Do, Zollinger, Winterhalter, & Cuenod, 1989; Zangerle, Cuenod, Winterhalter, & Do, 1992). An excess of L-cysteine has shown to produce in vivo excitotoxicity (Karlsen, Grofova, Malthe-Sorenssen, & Fonnum, 1981). This excitotoxic effect of L-cysteine occurs in a fashion remarkably similar to those produced by overexcitation of NMDA receptors which produce excessive influxes of Ca^{2+} ions at glutamatergic synapses (Janaky, Varga, Hermann, Saransaari, & Oja, 2000). The affinity of L-cysteine for NMDA receptor is supported by the finding that both competitive and non-competitive inhibition of the NMDA receptor precludes increases in Ca^{2+} influx produced by L-cysteine supplementation (Olney, Zorumski, Price, & Labruyere, 1990; Gleixner et al., 2017). Though we do not have data directly showing that NAC produces similar excitotoxic effects to those described in L-cysteine, it is plausible that such an effect could occur with NAC in the present study. It is not unreasonable to conclude that an excess of extracellular cysteine produced by NAC supplementation could have similar excitotoxic and deleterious effects. Future work should evaluate this conclusion more specifically to elucidate

similarities and differences between mechanisms responsible for excitotoxicity in L-cysteine and NAC supplementation.

Future Directions for the Treatment of Cue-Induced Amphetamine Craving and Concluding Remarks

The results of the current study suggest that NAC is likely ineffective for attenuating cue-induced craving for amphetamine, despite previous demonstrations of its potential for attenuating cue-induced relapse to cocaine (Reichel et al., 2011) and cue-induced reinstatement to methamphetamine (Siemsen et al., 2019). More broadly, these findings suggest that treatments and therapeutics used to treat cue-induced craving during drug abstinence cannot take a one-size fits-all approach, potentially even for treating drugs of abuse within the same drug class (e.g. cocaine and amphetamine). Rather, it is critical that research continues to discover, develop, and refine treatments specific to amphetamine-use disorder.

One particular molecular pathway that merits further investigation relies on mGluR5-mediated long-term depression at glutamatergic synapses. Recent literature has shown evidence suggesting that mGluR5 inhibits presynaptic glutamate release via a retrograde signaling cascade involving endogenous cannabinoids (eCBs) and presynaptic type-1 cannabinoid receptors (CBr1) (Li et al., 2018). These characteristics and findings make mGluR5 another viable and potentially promising mechanism to target in the development of pharmaceutical interventions to treat amphetamine addiction and relapse. However, the development of medications targeting mGluR5 systems inevitably requires more substantial knowledge of the molecular and cellular underpinnings of exactly how this mGluR5-eCB-CBr1 signalling cascade modulates drug-seeking. Zhang et al. (2021) has suggested that the decrease in glutamatergic tone on mGluR2/3

and concomitant increase in synaptic glutmate release that occurs with extrasynaptic glutamate depletion is heavily tied to two eCBs expressed on the surface of neurons and astrocytes. As such, the modulation of eCB signalling may serve as one potential pathway for normalizing glutamate homeostasis and treating cue-induced amphetamine seeking (Navarette & Araque, 2008; Navarette, et al., 2013; Zhang et al. 2021).

In addition to the putative molecular targets described above, one other therapeutic developmental strategy could prove useful in developing effective treatments for amphetamine relapse. Namely, "reverse translational" strategies have grown in popularity and shown promise in the last several years. In these strategies, investigators take what has shown efficacy in clinical populations and use that to derive a valid animal model. One specific instance of this has been demonstrated by Venniro et al. (2018), in which the investigators sought to emulate one of the most effective therapeutic strategies that we have for clinical populations, namely, community-based approaches such as Alcoholics or Narcotics Anonymous. Here, following methamphetamine self-administration, the experimenters offered animals two choices during abstinence. One lever offered the same methamphetamine infusion which they had received during self-adminsitration. However, the other lever offered social reinforcement where a door would raise allowing the animal to briefly interact with a peer animal from the nearby operant chamber. They found that by offering the option of social interaction during abstinence to methamphetamine, animals profoundly chose to abstain from taking methamphetamine and chose to socialize with the peer. This effect carried over when tested during protracted withdrawal with animals still choosing the lever that previously offered social reinforcement over the lever that previously offered methamphetamine. Overall, these results show clear merit

in a similar reverse translational strategy being used for the development of therapeutic and behavioral interventions designed to treat relapse to amphetamine.

References

Abdolahi A, et al. (2010). Incubation of nicotine seeking is associated with enhanced protein kinase A-regulated signaling of dopamine- and cAMP-regulated phosphoprotein of 32 kDa in the insular cortex. *European Journal of Neuroscience, 31*, 733-741.

Ahmed SH, Koob GF. (1998). Transition from moderate to excessive drug intake: Change in hedonic set point. *Science, 282* (5387), 298-300.

Ahmed SH, Walker JR, Koob GF. (2000). Persistent increase in the motivation to take heroin in rats with a history of drug escalation. *Neuropsychopharmacology, 22,* 413-421.

Airavaara M, et al. (2011). Endogenous GDNF in ventral tegmental area and nucleus accumbens does not play a role in the incubation of heroin craving. *Addiction Biology, 16*, 261-272.

Arndt DL, Johns KC, Dietz ZK, Cain ME. (2015). Environmental condition alters amphetamine self-administration: Role of the mGluR5 receptor and schedule of reinforcement. *Psychopharmacology, 232,* 3741-3752.

Baker DA, et al. (2003). Neuroadaptations in cystine-glutamate exchange underlie cocaine relapse. *Nature Neuorscience, 6*, 743-749.

Baker DA, Xi ZX, Shen H, Swanson CJ, Kalivas PW. (2002). The origin and neuronal function of in vivo nonsynaptic glutamate. *Journal of Neuroscience, 22*, 9134-9141.

Barnes TD, Kubota Y, Hu D, Jin DZ, Graybiel AM. (2005). Activity of striatal neurons reflects dynamic encoding and recording of procedural memories. *Nature, 437,*1158- 1161.

Berman DE, Dudai Y. (2001). Memory extinction, learning anew, and learning the new: Dissocations in the molecular machinery of learning in cortex. *Science, 291*, 2417-2419.

Berridge K, Robinson T. (1998). What is the role of dopamine in reward: Hedonic learning, or incentive salience? *Brain Research Reviews, 28*, 309-369.

Bienkowski P, et al. (2004). Time-dependent changes in alcohol-seeking behaviour during abstinence. *European Journal of Neuropsychopharmacology, 14,* 355-360.

Bonson, KR, et al. (2002). Neural systems of cue-induced cocaine craving. *Neuropsychopharmacology, 26,* 376-386.

Bouton, M. (1994). Conditioning, remembering, and forgetting. *Journal of Experimental Psychology., 20*(3), 219.

Bowers MS, Kalivas PW. (2003). Forebrain astroglial plasticity is induced following withdrawal from repeated cocaine administration. *European Journal of Neuroscience*, *17*(6), 1273-1278.

Brandt, S.A., Taverna, E.C., & Hallock, R.M. (2014). A survey of nonmedical use of tranquilizers, stimulants, and pain relievers among college students: Patterns of use among users and factors related to abstinence in non-users. *Drug and Alcohol Dependence, 143*, 272-276.

Brown, S.A., Tapert, S.F., Granholm, E., & Delis, D.C. (2000). Neurocognitive functioning of adolescents: Effects of protracted alcohol use. *Alcohol: Clinical and Experimental Research, 24*, 164-171.

Cain ME, Denehy EF, & Bardo MT. (2008). Individual differences in amphetamine self-administration: The role of the central nucleus of the amygdala. *Neuropsychopharmacology, 33*(5), 1149-1161.

Capriles N, Rodaros D, Sorge RE, Stewart J. (2003). A role for the prefrontal cortex in stress- and cocaine-induced reinstatement of cocaine seeking in rats. *Psychopharmacology, 168*, 66-74.

Caprioli D, Venniro M, Zhang M, Bossert JM, Warren BL, Hope BT, Shaham Y. (2017). Role of dorsomedial striatum neuronal ensembles in incubation of methamphetamine craving after voluntary abstinence. *Journal of Neuroscience, 37*(4), 1014-1027.

Danbolt NC. (2001). Glutamate uptake. *Progress in neurobiology, 65*(1), 1-105.

Diamond JS, Jahr CE. (1997). Transporters buffer synaptically released glutamate on a submillisecond time scale. *Journal of Neuroscience, 17,* 4672-4687.

Doya, K. (2008). Modulators of decision making. *Nature Neuroscience, 11*, 410-416.

Everitt BJ, Robbins TW. (2005). Neural systems of reinforcement for drug addiction: From actions to habits to compulsion. *Nature Neuroscience, 8*(11), 1481-1489.

Garcia EJ, Cain ME. (2021). Isolation housing elevates amphetamine seeking independent of nucleus accumbens glutamate receptor adaptations. *European Journal of Neuroscience,* 1-15.

Gass JT, Chandler LJ. (2013). The plasticity of extinction: Contribution of the prefrontal cortex in treating addiction through inhibitory learning. *Frontiers in Psychiatry, 4,* 46.

Gleixner AM, Hutchison DF, Sanniro S, Bhatia TN, Leak LC, Flaherty PT, Wipf P, Brodsky JL, Leak RK. (2017). N-acetyl-L-cysteine protects astrocytes against proteotoxicity without recourse to glutathione. *Molecular Pharmacology, 92*(5), 564-575.

Goldstein RZ, Volkow ND. (2011). Dysfunction of the prefrontal cortex in addiction: Neuroimaging findings and clinical implications. *Nature Neuroscience Reviews, 12*, 652-669.

Grimm JW, Hope BT, Wise RA, Shaham Y. (2001). Incubation of cocaine craving after withdrawal. *Nature, 412*, 141.

Herman M, Jahr CE. (2007). Extracellular glutamate concentration in hippocampal slice. *Journal of Neuroscience, 27*, 9736-9741.

Hiranita T, Nawata Y, Sakimua K, Anggadiredga K, Yamamoto T. (2006). Suppression of methamphetamine-seeking behavior by nicotinic agonists. *Proceedings of the National Academy of Sciences, 103*(22), 8523-8527.

Hollander JA, Carelli RM. (2005). Abstinence from cocaine self-administration heightens neural encoding of goal-directed behaviors in the accumbens. *Neuropsychopharmacology, 30*, 1464-1474.

Janaky R, Varga V, Herman A, Saransaari P, Oja SS. (2000). Mechanisms of L-cysteine neurotoxicity. *Neurochemical Research, 25*(9), 1397-1405.

Kalivas, P.W. (2009). The glutamate homeostasis hypothesis of addiction. *Nature reviews, 10*(8), 561-572.

Kalivas PW. (2007). Cocaine and amphetamine-like psychostimulants: Neurocircuitry and glutamate neuroplasticity. *Dialogues in Clinical Neuroscience, 9*(4), 389-397.

Kariisa, M., Scholl, L., Wilson, N., Seth, P., & Hoots, B. (2019). Drug overdose deaths involving cocaine and psychostimulants with abuse potential - United States, 2003-2017. *Morbidity and Mortality Weekly Report*, *68*(17), 388-395.

Karlsen RL, Grofovva I, Malthe-Sorenssen D, Fonnum F. (1981). Morphological changes in rat brain induced by L-cysteine injection in newborn animals. *Brain Research, 208,* 167-180.

Keller HJ, Do KQ, Zollinger M, Winterhalter KH, Cuenod M. (1989). Cysteine: Depolarization-induced release from rat brain in vitro. *Journal of Neurochemistry, 52*, 1801-1806.

Kelley AE. (2004). Memory and addictions: Shared neural circuitry and molecular mechanisms. *Neuron, 44*, 161-179.

Knackstedt L, LaRowe S, Mardikian P, Malcolm R, Upadhyaya H, Hedden S, Markou A, Kalivas PW. (2009). The role of cystine-glutamate exchange in nicotine dependence in rats and humans. *Biological Psychiatry, 65*(10), 841-845.

Knackstedt, L. A., Melendez, R. I., & Kalivas, P. W. (2010). Ceftriaxone restores glutamate homeostasis and prevents relapse to cocaine seeking. *Biological psychiatry*, *67*(1), 81–84.

Kousik SM, Napier TC, Carvey PM. (2012). The effects of psychostimulant drugs on blood brain barrier function and neuroinflammation. *Frontiers in Pharmacology, 3*, 121.

Lasseter HC, et al. (2010). Prefrontal cortical regulation of drug seeking in animal models of drug relapse. *Current Topics in Behavioral Neuroscience, 3*, 101-117.

Lu L, et al. (2004). Cocaine seeking over extended withdrawal periods in rats: Different time courses of responding induced by cocaine cues versus cocaine priming over the first 6 months. *Psychopharmacology, 176,* 101-108.

Ma YY, Lee BR, Wang X, Guo C, Lie L, Cui R, et al. (2014). Bidirectional modulation of incubation of cocaine craving by silent synapse-based remodeling of prefrontal cortex to accumbens projections. *Neuron, 83*(6), 1453-1467.

McFarland K, Kalivas PW. (2001). The circuitry mediating cocaine-induced reinstatement of drug-seeking behavior. *Journal of Neuroscience, 21*(21), 8655–8663.

McFarland K, Lapish CC, Kalivas PW. (2003). Prefrontal glutamate release into the core of the nucleus accumbens mediates cocaine-induced reinstatement of drug-seeking behavior. *Journal of Neuroscience, 23*(8), 3531-3537.

McFarland K, Lapish CC, Kalivas PW. (2003). Prefrontal glutamate release into the core of the nucleus accumbens mediates cocaine-induced reinstatement of drug-seeking behavior. *Journal of Neuroscience, 23*(8), 3531-3537.

Mogenson, G. J., Jones, D. L., & Yim, C. Y. (1980). From motivation to action: functional interface between the limbic system and the motor system. *Progress in neurobiology*, *14*(2-3), 69–97.

Monti PM, MacKillop J. (2007). Advances in the treatment of craving for alcohol and tobacco. In, P. M. Miller and D. Kavanaugh, Eds. *Translation of Addiction Science into Practice, Elsevier Science,* New York, p. 211-237.

Moorman DE, James MH, McGlinchey EM, Aston-Jones G. (2015). Differential roles of medial prefrontal subregions in the regulation of drug seeking. *Brain Research, 1628*, 130-146.

Moran MM, McFarland K, Melendez RI, Kalivas PW, Seamans JK. (2005). Cystine/glutamate exchange regulates metabotropic glutamate receptor presynaptic inhibition of excitatory transmission and vulnerability to cocaine seeking. *Journal of Neuroscience, 25*, 6389-6393.

Moussawi K, Pacchioni A, Moran M, Foster Olive M, Gass JT, Lavin A, Kalivas PW. (2009). N-acetylcysteine reverses cocaine-induced metaplasticity. *Nature Neuroscience, 12*(2), 182-189.

Murray JE, Lacoste J, Belin D. (2012). N-acetylcysteine as a treatment for addiction.

National Drug Intelligence Center. National Drug Threat Assessment. Washington, DC: United States Department of Justice; 2012.

Olney JW, Zorumski C, Price MT, Labruyere J. (1990). L-cysteine, a bicarbonate-sensitive endogenous excitotoxin. *Science, 248,* 596-599.

Pelloux Y, Murray JE, Everitt BJ. (2013). Differential roles of the prefrontal cortical subregions and basolateral amygdala in compulsive cocaine seeking and relapse after voluntary abstinence in rats. *European Journal of Neuroscience, 38*, 3018-3026.

Pendyam S, Mohan A, Kalivas PW, Nair SS. (2009). Computational model of extracellular glutamate in the nucleus accumbens incorporates neuroadaptations by chronic cocaine. *Neuroscience, 158*, 1266-1276.

Peters J, LaLumiere RT, Kalivas PW. (2008). Infralimbic prefrontal cortex is responsible for inhibiting cocaine seeking in extinguished rats. *Journal of Neuroscience, 28*(23), 6046-6053.

Pickens CL, Airavaara M, Theberge F, Fanous S, Hope BT, Shaham Y. (2011). Neurobiology of the incubation of drug craving. *Trends in Neuroscience, 34*(8), 411-420.

Reichel CM, Moussawi K, Do PH, Kalivas PW, See RE. (2011). Chronic N-acetylcysteine during abstinence or extinction after cocaine self-administration produces enduring reductions in drug seeking. *The Journal of Pharmacology and Experimental Therapeutics, 337*(2), 487-493.

Ritz MC, Lamb RJ, Goldberg SR, Kuhar MJ. (1987). Cocaine receptors on dopamine transporters are related to self-administration of cocaine. *Science, 237,* 1219-1223.

Sari, Y., Smith, K. D., Ali, P. K., & Rebec, G. V. (2009). Upregulation of GLT1 attenuates cue-induced reinstatement of cocaine-seeking behavior in rats. *The Journal of Neuroscience*, *29*(29), 9239–9243.

Seiden LS, Sabol KE, Ricaurte GA. (1993). Amphetamine: Effects on catecholamine systems and behavior. *Annual Review of Pharmacology and Toxicology, 33,* 639-677.

Sesack, S. R., & Grace, A. A. (2010). Cortico-Basal Ganglia reward network: microcircuitry. *Neuropsychopharmacology : official publication of the American College of Neuropsychopharmacology*, *35*(1), 27–47.

Shalev U, et al. (2001). Time-dependent changes in extinction behavior and stress-induced reinstatement of drug seeking following withdrawal from heroin in rats. *Psychopharmacology, 156,* 98-107.

Simesen BM, et al. (2019). Effects of methamphetamine self-administration and extinction on astrocyte structure and function in the nucleus accumbens core. *Neuroscience, 406*, 528-541.

Sulzer, D., Maidment, N. T., & Rayport, S. (1993). Amphetamine and other weak bases act to promote reverse transport of dopamine in ventral midbrain neurons. *Journal of neurochemistry*, *60*(2), 527–535.

Swinford-Jackson SE, Anastasio NC, Fox RG, Stutz SJ, Cunningham KA. (2016). Incubation of cocaine cue reactivity associates with neuroadaptions in the cortical serotonin (5-HT) 5-HT2C receptor system. *Neuroscience, 324,* 50-61.

Timmerman W, Westerink BH. (1997). Brain microdialysates of GABA and glutamate: What does it signify? *Synapse, 27*, 242-261.

Van den Oever MC, Spijker S, Smit AB, De Vries TJ. (2010). Prefrontal cortex plasticity mechanisms in drug seeking and relapse. *Neuroscience and Biobehavioral Reviews, 35*(2), 276-284.

Venniro M., Zhang M., Caprioli D. *et al.* (2018). Volitional social interaction prevents drug addiction in rat models. *Nature Neurosci 21*, 1520–1529.

Vertes RP. (2004). Differential projections of the infralimbic and prelimbic cortex in the rat. *Synapse, 51*, 32-58.

Vertes RP. (2006). Interactions among the medial prefrontal cortex, hippocampus and midline thalamus in emotional and cognitive processing in the rat. *Neuroscience, 142*, 1-20.

Volkow ND, et al. (2010). Cognitive control of drug craving inhibits brain reward regions in cocaine abusers. *Neuroimage, 49,* 2536-2543.

Weissenborn R, Robbins TW, Everitt BJ. (1997). Effects of medial prefrontal or anterior cingulate cortex lesions on responding for cocaine under fixed-ratio and second-order schedules of reinforcement in rats. *Psychopharmacology, 134*, 242-257.

White, F. J., Wachtel, S. R., Johansen, P. A., & Einhorn, L. C. (1987). Electrophysiological studies of the rat mesoaccumbens dopamine system: Focus on dopamine receptor subtypes, interactions, and the effects of cocaine. *Neurophysiology of Dopaminergic Systems-Current Status and Clinical Perspectives. Grosse Point, Ml: Lakeshore*, 317-365.

Wolf ME. (2016). Synaptic mechanisms underlying persistent cocaine craving. *Nature Reviews, 17,* 351-365.

Yalachkov, Y, Kaiser J, Naumer MJ. (2009). Brain regions related to tool use and action knowledge reflect nicotine dependence. *Journal of Neuroscience, 29*, 4922-4929.

Yin HH, Knowlton BJ. (2007). The role of the basal ganglia in habit formation. *Nature Reviews, 7*, 464-476.

Zangerle L, Cuenod M, Winterhalter KH, Do KQ. (1992). Screening of thiol compounds: Depolarization-induced release of glutathione and cysteine from rat brain slices. *Journal of Neurochemistry, 59,* 18